Article

Structure

Dual Site Phosphorylation of Caspase-7 by PAK2 Blocks Apoptotic Activity by Two Distinct Mechanisms

Graphical Abstract

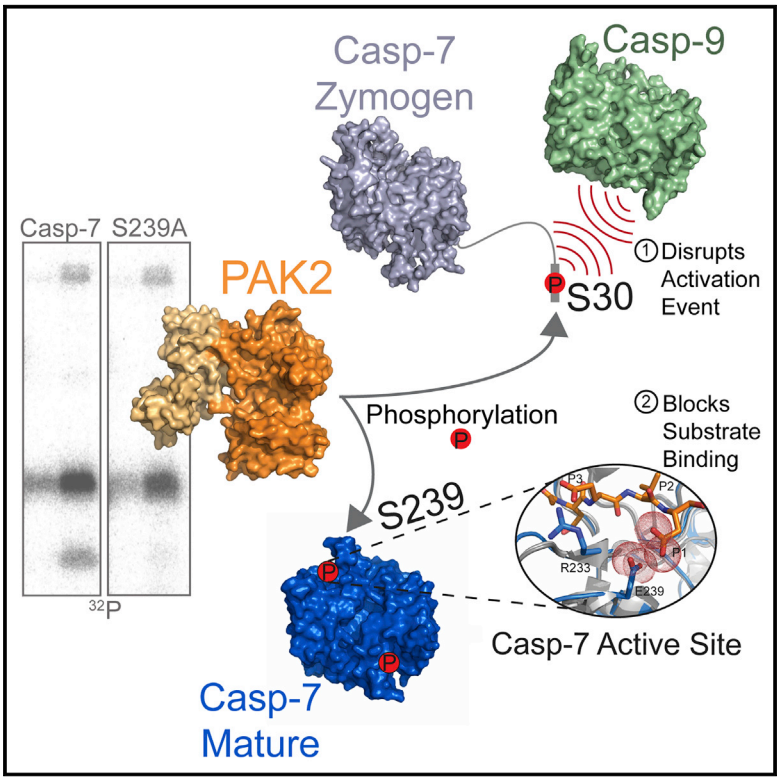

Highlights

- PAK2 phosphorylation of caspase-7 inhibits activity by two distinct mechanisms
- Phosphorylation of caspase-7 at S30 slows zymogen activation by upstream caspases
- S30 phosphorylation interferes with caspase-7:caspase-9 interaction
- Crystal structure of S239E phosphomimetic suggests substrate binding is obstructed

Authors

Scott J. Eron, Kishore Raghupathi, Jeanne A. Hardy

Correspondence

hardy@chem.umass.edu

In Brief

PAK2 phosphorylates caspase-7 resulting in loss of activity, which is implicated in resistance to chemotherapeutic agents. Eron et al. decipher the molecular mechanism of phosphorylated caspase-7 inhibition at two phosphorylation sites. Phosphorylation at S30 slows initial activation while phosphorylation at S239 blocks substrate binding.

Accession Numbers

5K20

Eron et al., 2017, Structure *25*, 1–13
January 3, 2017
http://dx.doi.org/10.1016/j.str.2016.11.001

CellPress

Please cite this article in press as: Eron et al., Dual Site Phosphorylation of Caspase-7 by PAK2 Blocks Apoptotic Activity by Two Distinct Mechanisms, Structure (2016), http://dx.doi.org/10.1016/j.str.2016.11.001

Structure
Article

Dual Site Phosphorylation of Caspase-7 by PAK2 Blocks Apoptotic Activity by Two Distinct Mechanisms

Scott J. Eron,[1] Kishore Raghupathi,[1] and Jeanne A. Hardy[1,2,*]
[1]Department of Chemistry, University of Massachusetts Amherst, 104 LGRT, 710 North Pleasant Street, Amherst, MA 01003, USA
[2]Lead Contact
*Correspondence: hardy@chem.umass.edu
http://dx.doi.org/10.1016/j.str.2016.11.001

SUMMARY

Caspases, the cysteine proteases that execute apoptosis, are tightly regulated via phosphorylation by a series of kinases. Although all apoptotic caspases work in concert to promote apoptosis, different kinases regulate individual caspases. Several sites of caspase-7 phosphorylation have been reported, but without knowing the molecular details, it has been impossible to exploit or control these complex interactions, which normally prevent unwanted proliferation. During dysregulation, PAK2 kinase plays an alternative anti-apoptotic role, phosphorylating caspase-7 and promoting unfettered cell growth and chemotherapeutic resistance. PAK2 phosphorylates caspase-7 at two sites, inhibiting activity using two different molecular mechanisms, before and during apoptosis. Phosphorylation of caspase-7 S30 allosterically obstructs its interaction with caspase-9, preventing intersubunit linker processing, slowing or preventing caspase-7 activation. S239 phosphorylation renders active caspase-7 incapable of binding substrate, blocking later events in apoptosis. Each of these mechanisms is novel, representing new opportunities for synergistic control of caspases and their counterpart kinases.

INTRODUCTION

Tens of billions of cells die each day by the controlled cell death pathways of apoptosis. Apoptotic programmed cell death is fundamental for all multicellular eukaryotes and is critical for organismal development, differentiation, eliminating damaged cells, and maintaining homeostasis. Dysregulation of apoptosis has been linked to diseases including cancer (Greenblatt et al., 1994; Pistritto et al., 2016; Plati et al., 2010; Vaux et al., 1988), autoimmune disorders (Worth et al., 2006), and neurodegeneration (Ghavami et al., 2014; Margolis et al., 1994). In particular, transformation to a cancerous phenotype occurs when cells establish barriers to apoptosis and develop resistance to signals designed to eliminate malignant abnormalities via apoptosis.

The apoptotic cascade is ultimately dependent on the activation of the caspase family of cysteine proteases. These enzymes dismantle the cell by cleaving a diverse set of protein substrates (Dix et al., 2008) with a specificity for acidic residues, typically aspartate, at the P1 position (Stennicke et al., 2000) although glutamate (Moretti et al., 2002) and phosphoserine can also be recognized (Seaman et al., 2016). Apoptotic caspases are divided into two classes: the initiator caspases (caspase-8, -9, and -10) and their substrates, the executioner caspases (caspase-3, -6, and -7), which cleave specific cellular targets to invoke cell death. Caspases are functional as homodimers, with each monomer made up of an N-terminal prodomain, one large and one small subunit (Figure 1A). As a means of inherent regulation, executioner caspases are translated as inactive procaspase zymogens, with distinct cleavage events required for zymogen activation. Initiator caspases propagate the apoptotic signal by cleaving downstream executioner caspases at their intersubunit linker. Prior to cleavage, this linker rests across the dimer interface (Riedl et al., 2001). Cleavage of the intersubunit linker generates loops 2 and 2′ (L2 and L2′), which, in the active, substrate-bound conformation, lock together the substrate-binding groove on the opposite monomer (Figure 1B) (Witkowski and Hardy, 2009). This results in a dramatic conformational change in the dynamic active-site loop bundle from a zymogen state to an active state. Cleaved executioners can also experience a reversal to the zymogen-like state by small molecules (Hardy et al., 2004), which forces a loop rearrangement that traps L2′ over the dimer interface and results in the expulsion of loop 3 from the active-site pocket. Following activation in the cell, each executioner caspase cleaves over 100 substrates (Agard et al., 2012; Hill et al., 2016) to propagate the well-ordered termination of the dying cell.

Due to their cell-death-inducing potential, caspase activation and downstream activity is tightly regulated on multiple levels, with phosphorylation as one of the primary means to manage apoptotic caspase activity (Allan and Clarke, 2007; Alvarado-Kristensson et al., 2004; Andersen et al., 2009; Cardone et al., 1998; Li et al., 2011; McDonnell et al., 2008; Suzuki et al., 2004). In fact, caspases and kinases co-regulate each other, resulting in an intricate interplay of dramatic posttranslational modifications that ultimately affect cell death and survival (Dix et al., 2012; Kurokawa and Kornbluth, 2009; Zukowski and Litchfield, 2015). Together, apoptotic caspases are recognized to initiate and execute cell death, but their individual roles continue to come to light. Even highly related caspases play non-overlapping

Please cite this article in press as: Eron et al., Dual Site Phosphorylation of Caspase-7 by PAK2 Blocks Apoptotic Activity by Two Distinct Mechanisms, Structure (2016), http://dx.doi.org/10.1016/j.str.2016.11.001

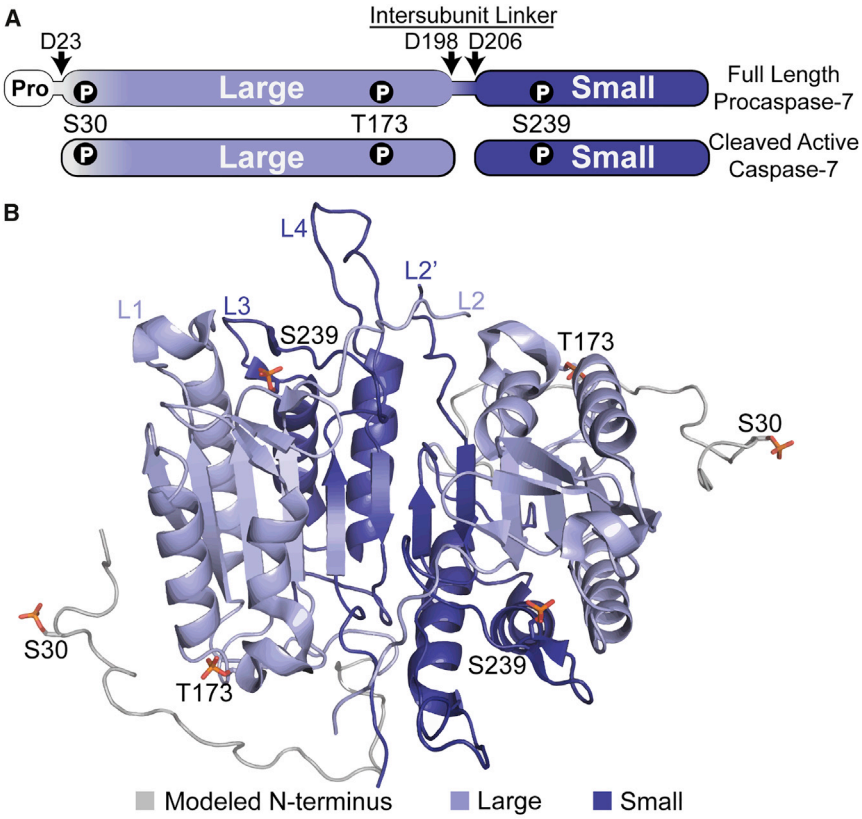

C

Caspase-7	K_M (μM)	k_{cat} (s^{-1})	k_{cat} / K_M ($\times 10^2$ $\mu M^{-1} s^{-1}$)
Wild Type	61 ± 9.5	6.1 ± 0.21	9.9
S30E	63 ± 6.2	4.5 ± 0.19	7.2
T173E	57 ± 13	3.9 ± 0.37	6.9
S239E	730 ± 210	0.073 ± 0.017	0.010
S239Q	360 ± 32	2.3 ± 0.071	0.60
S239D	680 ± 78	1.5 ± 0.088	0.20

Figure 1. Sites of Caspase-7 Phosphorylation by PAK2 and Kinetics of Phosphomimetic Variants

(A) Domain structure of caspase-7 highlighting the three reported sites of phosphorylation by PAK2 as Ⓟ. Caspase-7 is cleaved and thereby activated by upstream initiator caspases (cleavage sites indicated by arrows). The full-length procaspase-7 dimer is processed to remove the prodomain, and at the intersubunit linker to form the large (light blue) and small (dark blue) subunits making active, cleaved caspase-7.

(B) Three phosphorylation sites (orange sticks) are present in the caspase-7 dimer consisting of two large (light blue) and small (dark blue) subunits. The N terminus of active caspase-7, which is dynamic and unstructured, has not been resolved crystallographically, so a model of the S30 region has been added (gray). The prodomain (residues 1–23) is not shown. S239 sits below the active site in loop 3 and T173 rests at the bottom of the 160's helix. The active site of caspase-7 is composed of four loops from one half of the dimer (L1, L2, L3, L4) and one loop from the opposite half of the dimer (L2′).

(C) Kinetic data of phosphomimetic variants. Substitution at S239, but at no other reported phosphorylation site, has a dramatic effect on caspase-7 activity.

biological roles and are independently regulated by inhibitor proteins, zinc, and posttranslational modifications (Dagbay et al., 2014). Interactions with kinases are a major contribution to the unique regulation of individual caspases. The delicate nature of this balance between caspases and kinases has been exploited by a number of cancers (Allan et al., 2003; Cursi et al., 2006), which have developed resistance to apoptosis, even after stimulation by chemotherapeutic agents (Li et al., 2011; Marlin et al., 2009).

Many cancers have capitalized on the vast signaling capacity of various kinases to manipulate cell processes (Dhillon et al., 2007). One particular example is the dysregulation of p21-activated kinase 2 (PAK2, γ-PAK) (Dummler et al., 2009; Mira et al., 2000). PAK2, the only ubiquitously expressed PAK, plays a role in a variety of biological pathways, including cell motility, mitosis, survival, and apoptosis. Interestingly, PAK2 plays a dual role in the context of apoptosis: active full-length PAK2 stimulates cell survival (Jakobi et al., 2001; Marlin et al., 2009) while cleavage of the autoinhibitory domain results in propagation of the pro-apoptotic response (Lee et al., 1997; Rudel and Bokoch, 1997). This duality is dictated by the relationship of PAK2 with caspase cleavage (Marlin et al., 2011). PAK2 is cleaved by the executioner caspase-3 at D212, which separates the PAK2 kinase domain and autoinhibitory domains (Walter et al., 1998). The phosphorylated kinase domain, PAK2p34, is then translocated to the nucleus (Jakobi et al., 2003) where it phosphorylates a new set of substrates, which in turn promote programmed cell death. A number of breast cancer cell lines have shown hyperactivity of PAK2 (Mira et al., 2000), which tips the scale to favor full-length PAK2 and results in reduced levels of apoptosis. Full-length, active PAK2 stimulates cell survival through multiple mechanisms, including caspase phosphorylation (Li et al., 2011). This overactivity has further been linked to resistance to chemotherapeutic agents.

The complexity of the caspase-kinase crosstalk has been intensified with the discovery that a pathway involving PAK2 is able to phosphorylate the executioner caspase-7 at three distinct residues: S30, T173, and S239 (Li et al., 2011). Although PAK2 and caspase-7 co-localize and co-immunoprecipitate, whether this phosphorylation of caspase-7 is mediated by PAK2 directly or by another kinase in that pathway was not fully elucidated by prior work. Phosphorylation of all three residues S30, T173, and S239 is reported to silence caspase-7 enzymatic

activity, but the contribution from each individual site has not been studied nor has the mechanism of inhibition been determined. As a result of a total loss in caspase-7 activity, phosphorylation by PAK2 leads to a reduction in apoptosis. In addition, knockdowns of PAK2 in various breast cancer cell lines lead to increased apoptosis levels when stimulated with chemotherapeutics, including staurosporine or doxorubicin (Li et al., 2011), underscoring that PAK2 is critical in curtailing caspase-7 activity.

Here, we elucidate the molecular mechanism by which PAK2 phosphorylation inhibits caspase-7 function. Understanding the regulation of this executioner caspase has implications in cancer resistance and apoptotic activation. Our results show that PAK2 inhibits caspase-7 by two divergent mechanisms prior to and following caspase activation: initial phosphorylation allosterically slows activation by upstream initiator caspases by impeding cleavage at the intersubunit linker and a second phosphorylation site directly blocks substrate binding. Identifying and resolving the molecular mechanism behind both regulatory phosphorylation events provides valuable insight into therapeutically relevant means to control programmed cell death.

RESULTS

The S239E Phosphomimetic Inactivates Caspase-7

Phosphorylation of caspase-7 by a PAK2-dependent pathway inactivates caspase-7, and this appears to attenuate apoptosis in several breast cancers after stimulation by chemotherapeutic agents (Li et al., 2011). Caspase-7 phosphorylation by PAK2 occurs at three sites: S30, T173, and S239 (Figure 1A), but the impact of phosphorylation at these individual sites on caspase-7 function or their mechanisms of regulating caspase-7 have not been investigated. Prior to activation, caspase-7 exists as a zymogen. Proteolytic cleavage by upstream initiator caspases at the prodomain (D23) and the intersubunit linker (D198/D206) generates the active form of caspase-7 comprising large and small subunits of caspase-7 (Figure 1B). In the small subunit, S239 sits below the substrate-binding groove on loop 3, which is part of the active-site loop bundle. T173 is located at the bottom of the 160's helix, whereas S30, in the highly mobile N-terminal region, has not been resolved by any caspase-7 crystal structures.

To explore the impacts of phosphorylation, each of the three reported phosphorylation sites were replaced by glutamate to generate phosphomimetic variants, mirroring the negative charge and steric bulk of phosphoserine or phosphothreonine. To ensure that activity was monitored in a cleaved (active) form, each phosphomimetic was expressed from a constitutively two-chain construct in which the large and small subunits are independently expressed (Witkowski and Hardy, 2011). Neither S30E nor T173E had a significant effect on caspase-7 kinetics (Figure 1C). However, S239E had a dramatic effect on caspase-7 activity, dropping the catalytic efficiency by nearly three orders of magnitude compared with the wild-type enzyme.

The introduction of negative charges in combination with steric bulk are two attributes that enable phosphorylation to have such significant effects on protein function. We next aimed to determine whether size, charge, or both, were responsible for the S239E loss of activity. Substituting S239 with Gln retains the size of the Glu but removes the contribution of a negative charge. Conversely, the S239D variant retains the negative charge but removes the bulk. Both S239Q and S239D resulted in a significant drop in catalytic efficiency, but neither as dramatic as S239E, suggesting that both size and charge play a large role in inhibiting caspase-7 activity at S239. Notably, all three mutations (S239E, S239D, and S239Q) had a significant effect on K_M, highly suggesting that phosphorylation at S239 interferes directly in a steric manner with substrate binding. In addition, there was an effect on k_{cat} for the S239E mutation, suggesting a disruption to the catalytic machinery. However, this k_{cat} effect was much less pronounced with the Gln and Asp mutations, further suggesting that both size and charge together are responsible for inhibition.

Caspase-7 Is Phosphorylated by PAK2 at S239 on the Small Subunit

To investigate PAK2 phosphorylation of the caspase-7 small subunit, which contains S239, we performed an in vitro phosphorylation assay. PAK2 T402E, a constitutively active, autoactivating variant was pre-activated with ATP then incubated with [γ-^{32}P]ATP and wild-type caspase-7 or the S239A variant, which cannot be phosphorylated at residue 239 (Figure 2A). Based on the low activity of S239E, we anticipated phosphorylation on the small subunit. We observed active caspase-7 completely cleaved PAK2 at D212 (Figures 2A and S1) to generate the kinase and autoinhibitory domains. In addition, in both the wild-type caspase-7 and S239A reactions, a phosphorylated band similar in molecular weight to the small subunit of caspase-7 appeared. To determine whether this 14 kDa band was a cleavage product of PAK2 or the small subunit of caspase-7, we repeated the in vitro phosphorylation assay on catalytically inactive caspase-7 (C186A, Figure 2B), which was expressed using the constitutively two-chain construct. PAK2 cannot be cleaved by inactive caspase-7 C186A. The lack of the 14 kDa band with inactive caspase-7 confirms that the band is indeed a cleavage product of PAK2. Contrary to our expectations, we did not observe small subunit phosphorylation under these conditions.

These results demonstrate the difficulty in dissecting the competitive interplay between caspase-7 and PAK2. If active caspase-7 predominates, it cleaves PAK2 before PAK2 can phosphorylate the caspase-7 small subunit, which inactivates caspase-7. We sought a reagent that could block caspase-7 activity thereby preventing cleavage of PAK2. Due to the location of S239, it was important that the reagent not fill the substrate-binding groove and thereby limit accessibility of S239. To meet these criteria, we developed a cysteine-protecting group (PG, L-cysteinyl-2-pyridyl disulfide; Figure S2A). PG (Figure S2B) modifies and inactivates the catalytic cysteine via reversible thiol chemistry (Ventura et al., 2015), but because of its small size, does not fill the full substrate-binding groove. In the presence of PG, PAK2 clearly phosphorylated the small subunit of wild-type caspase-7 at S239, since no phosphorylation of S239A was observed (Figure 2C). In addition, the PAK2 remains uncleaved, and the large subunit of caspase-7 is phosphorylated at the same levels as with unprotected caspase-7, demonstrating that S239 can indeed be phosphorylated by PAK2.

In addition to silencing the caspase-7 activity, the PG plays an orthogonal role at a second site, altering the equilibrium

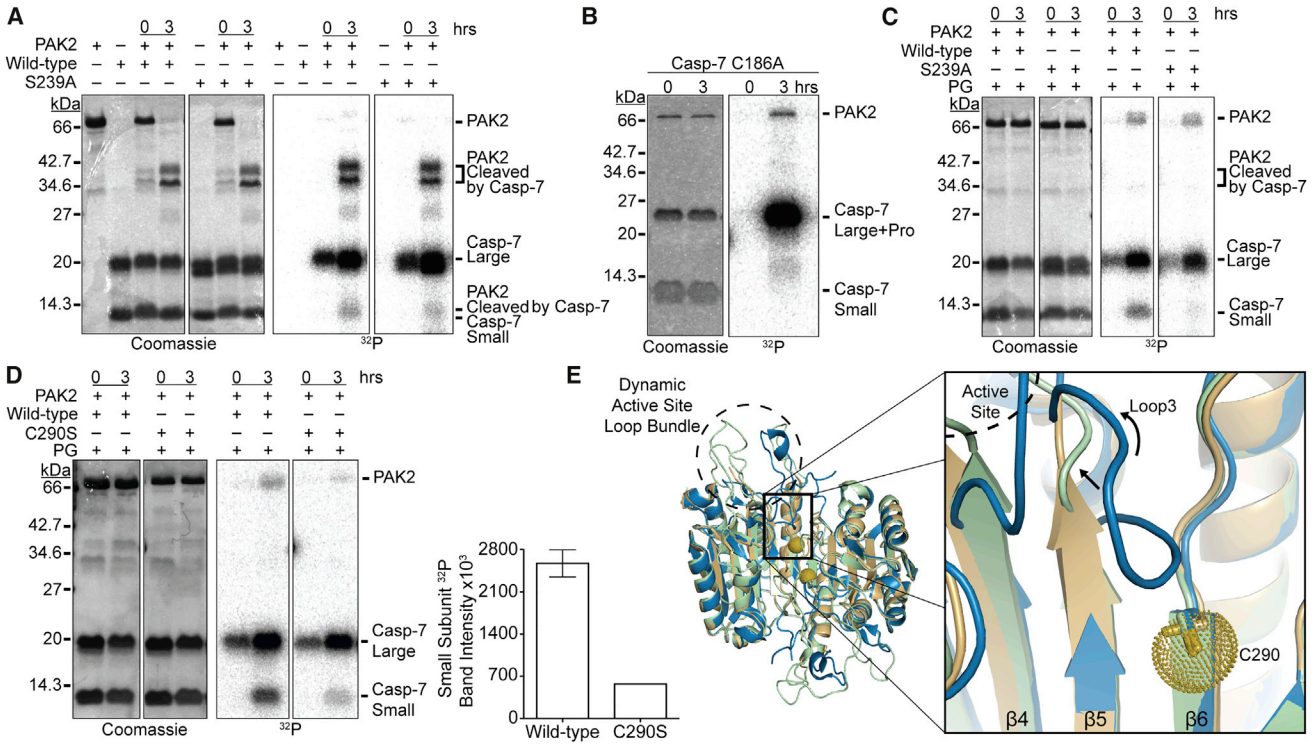

Figure 2. PAK2 Phosphorylates the Caspase-7 Small Subunit at S239

(A) PAK2 phosphorylates caspase-7 at multiple sites as assessed by autoradiography by [γ-^{32}P]ATP and comparison to Coomassie-stained gels. The caspase-7 large subunit is phosphorylated rapidly, with phosphorylation observed even before the zero time point could be analyzed. PAK2 autophosphorylation indicates that PAK2 is active. After 3 hr, PAK2 is cleaved by caspase-7 resulting in multiple bands of cleaved PAK2.

(B) PAK2 phosphorylates catalytically inactive caspase-7 (C186A) at the large subunit. Because caspase-7 is not active, no cleaved PAK2 is observed.

(C) After incubation with a cysteinyl-2-pyridyl disulfide protecting group (PG), which blocks the catalytic cysteine, caspase-7 can be phosphorylated by PAK2 on both the large and small subunits. Substituting S239 (small subunit) with alanine results in the complete loss of caspase-7 phosphorylation on the small subunit, confirming PAK2 phosphorylates the caspase-7 small subunit at S239.

(D) After incubation with the PG, both the wild-type caspase-7 and C290S are phosphorylated by PAK2 on the large subunit. The C290S variant prevents PG binding to this C290, which has known allosteric implications. Serine substitution at C290 results in a dramatic loss in small subunit phosphorylation at S239 by PAK2. The band intensity for small subunit phosphorylation is quantified in the bar graph on the right, which shows the mean ± error represented as SD from three independent experiments.

(E) The dynamic loop bundle at the active site can adopt different conformations. Alignment of three crystal structures reveals that unliganded caspase-7 (blue, PDB: 3IBF) is distinct from the full-length procaspase-7 (green, PDB: 1GQF) and from caspase-7 bound to the allosteric inhibitor DICA (tan, PDB: 1SHJ). In all three conformations, C290 sits on β strand 6, however, the base of loop 3 is in a dramatically different conformation. The unliganded structure loses β-character in β5 while both the full-length procaspase-7 zymogen and the DICA-bound structures extend β5 and expel loop 3 from this allosteric pocket at the dimer interface. Binding PG at C290 provides considerable steric bulk that is expected to force loop 3 of the unliganded caspase-7 (blue loop 3) to adopt a loop-accessible conformation (tan loop 3) as seen when DICA binds at this cysteine, C290.

In all parts of this figure, all caspase-7 variants were expressed from the constitutively two-chain construct, which produces the large (1–198) and small (199–303) subunits of caspase-7 as two independent polypeptides.

ensemble of the active-site loops by binding to a known allosterically acting cysteine (C290). Upon activation by cleavage at the intersubunit linker, caspase-7 experiences a rearrangement of its loops, which sample multiple conformations. For example, caspase-7 bound to the small molecule DICA (at C290) forces loop 3 to adopt a more accessible conformation, with an increased exposure to solvent. We realized that binding of the PG at C290 should increase the accessibility of this region by forcing loop 3 into a more accessible conformation. To test this hypothesis, we mutated C290 to Ser, blocking the ability of the PG to bind at the allosteric Cys. We observed a decrease in phosphorylation on the small subunit of caspase-7 C290S compared with wild-type (Figure 2D). We did not observe a similar decrease when C186 was mutated to Ala (Figure S3), suggesting that PG binding to C290, but not C186, was responsible for loop movement and availability of S239 to phosphorylation by PAK2.

Thus, it appears that PG binding to C290 acts analogously to binding of other small molecules at C290, resulting in a structural change to loop 3 (Figure 2E). In unliganded caspase-7 (Figure 2E, blue), loop 3 is structured and protrudes inwards toward C290. When a small molecule like DICA or PG binds at C290, loop 3 is forced upward in a loop-accessible conformation that may resemble the zymogen full-length procaspase-7 (Figure 2E, green) or caspase-7 bound to DICA (Figure 2E, tan). This conformational shift increases the solvent accessibility of loop 3, including S239. The PG thus served two purposes: (1) to silence caspase-7 activity allowing PAK2 to remain uncleaved so that

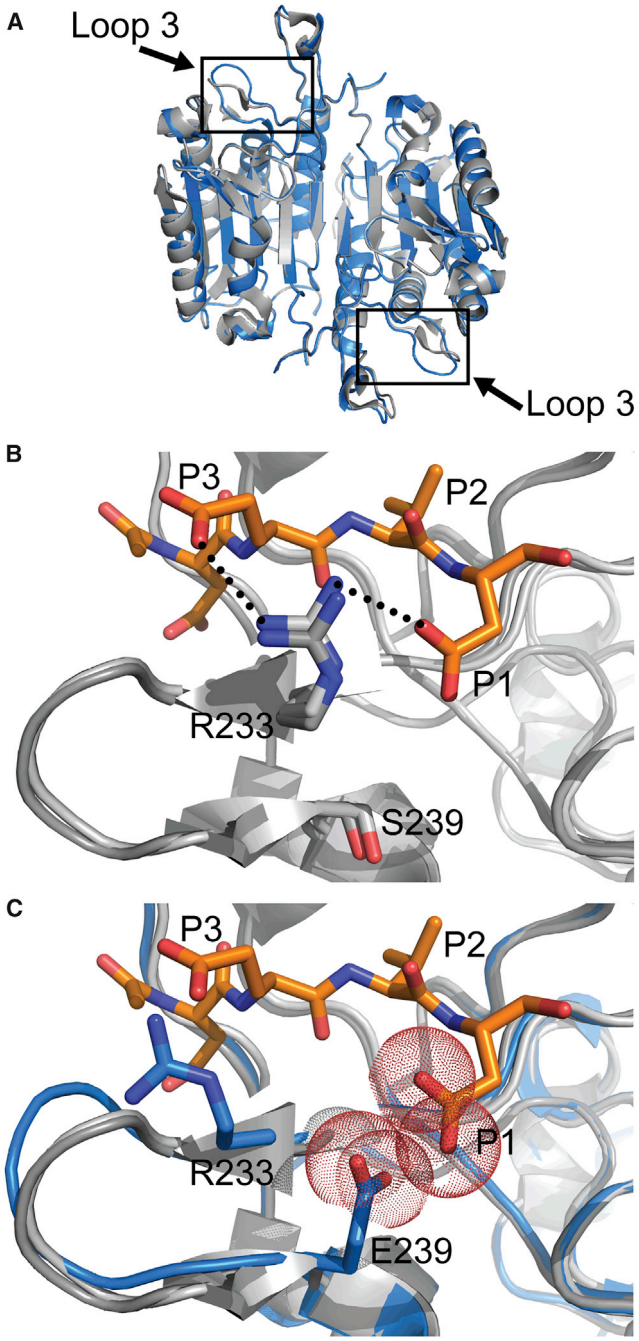

Figure 3. Phosphorylation at Caspase-7 S239 Sterically Blocks Substrate Binding

(A) Global alignment of the unliganded caspase-7 S239E phosphomimetic crystal structure (light blue) and the unliganded wild-type caspase-7 (dark gray, PDB: 3IBF). Loop 3, which contains the S239E mutation, undergoes a clear shift in conformation.

(B) R233 interactions are essential for substrate binding and specificity. In both active-site liganded (gray, PDB: 1F1J) and unliganded (dark gray, PDB: 3IBF) caspase-7 structures, R233 is positioned to form two of the essential side-chain hydrogen bonds (black dots) that are critical for binding substrate (DEVD, orange sticks), anchoring it in place for catalysis.

(C) The unliganded S239E phosphomimetic crystal structure (blue) shows a dramatic shift in loop 3, with the introduced glutamate forcing R233 out of the position compatible for binding substrate. In addition, the introduction of a negative charge in the P1 pocket would electrostatically repel an aspartate residue from the substrate.

phosphorylation can proceed and (2) to alter the equilibrium of the caspase-7 active-site loop bundle to favor the solvent-accessible conformation of loop 3, which includes the phosphorylation site S239. It is clear that phosphorylation of S239 occurs exclusively when loop 3 is in an exposed, loop-accessible conformation. This suggests either that S239 is only available for phosphorylation under certain conditions or that PAK2 can distinguish these two distinct conformations of caspase-7.

S239E Phosphomimetic Structure Suggests the Mechanism of Inhibition by Phosphorylation

To determine the molecular mechanism of inhibition by phosphorylation at S239, we solved the crystal structure of the unliganded (apo) cleaved form of the caspase-7 S239E phosphomimetic at 2.2 Å resolution (Table S1). This caspase-7 phosphomimetic shares the same overall fold with all previously crystallized caspase-7 structures, including those unbound and bound to substrate mimics. The heterotetrameric core consists of 12 β strands flanked by 10 α helices, and two symmetrical active sites made of dynamic active-site loop bundles. Loop 3 sits just below the active site and contains R233, a critical residue for binding substrate (Figure 3A). In both the unliganded mature structure (PDB: 3IBF) and the substrate-mimic bound structure (PDB: 1F1J), this arginine is positioned identically (Figure 3B). R233 acts as an anchor poised to make four pivotal hydrogen bonds with the preferred DEVD tetrapeptide substrate. R233 interacts with both the Glu in the P3 position of the peptide substrate as well as the essential Asp side chain in the P1 position. Meanwhile, two additional hydrogen bonds are made with the carbonyl and nitrogen stemming from the R233 backbone. This behavior of R233 is in contrast to its behavior in the S239E structure.

The structure of unliganded caspase-7 S239E suggests a two-factor mechanism by which phosphorylation of S239 inhibits caspase-7. First, the position of loop 3 has been perturbed by the phosphomimetic (Figure 3C). The bulk from the introduced Glu side chain at position 239, which mimics the phosphoserine in length and negative charge, forces the entire loop 3 to shift outward toward a solvent channel. This reorients R233 away from the active-site pocket so that it can no longer make critical bonds with the substrate (Figure 3C). In addition, the phosphomimetic introduces a negative charge in the precise region where an aspartate would bind in the S1 pocket. This inhibitory mechanism is consistent with the kinetic data (Figure 1C), which suggests both size (S239Q) and charge (S239D) work in combination to inhibit caspase-7 activity upon modification at S239. Thus, phosphorylation at S239 is effective at silencing the activity of an already active caspase-7 once apoptosis has been initiated.

Caspase-7 Phosphorylation Occurs on the Large Subunit Primarily at S30

Phosphorylation of caspase-7 by PAK2 was also observed on the large subunit (Figure 2). This phosphorylation event was so fast that it occurred before the zero time point sample could

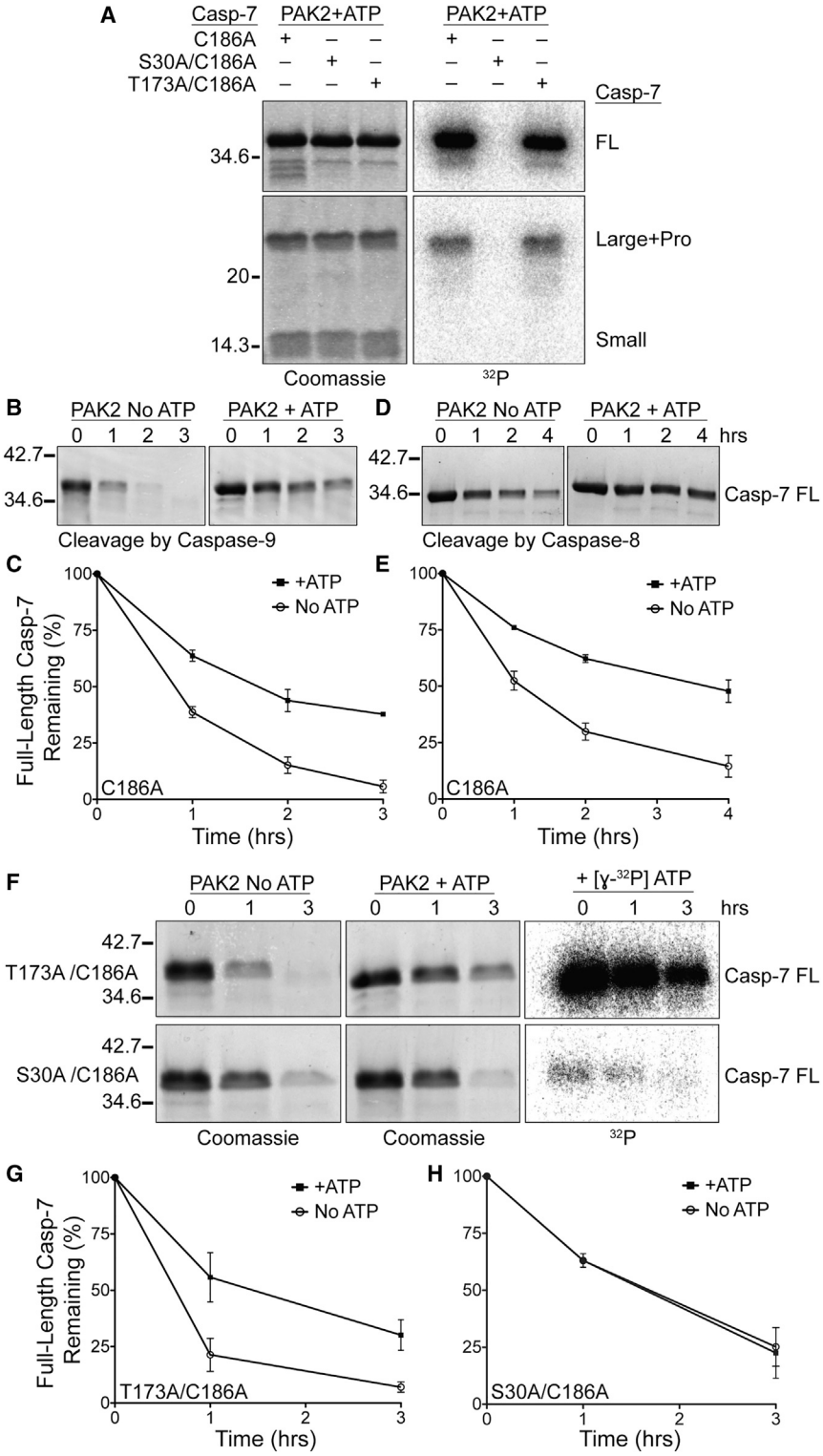

Figure 4. Phosphorylation at S30 on Caspase-7 Slows Processing by Upstream Initiator Caspases

(A) PAK2 phosphorylates the large subunit in both the full-length (FL) and in the cleaved states of caspase-7. The two reported phosphorylation sites in the large subunit were individually mutated to alanine. Lack of [γ-^{32}P]ATP labeling of S30A suggests that phosphorylation primarily occurs at S30 on the caspase-7 large subunit and not at T173. All caspase-7 constructs contain the C186A substitution of the catalytic cysteine to prevent self-cleavage. Cleavage was monitored by Coomassie-stained SDS-PAGE, and ^{32}P autoradiography was used to confirm phosphorylation.

(B and D) Cleavage of full-length (FL) caspase-7 by upstream initiators caspase-9 (B) or caspase-8 (D) at the intersubunit linker. The addition of ATP activates PAK2 and stimulates caspase-7 phosphorylation, which slows the ability of caspase-9 or caspase-8 to cleave FL caspase-7 at the intersubunit linker.

(C and E) Quantification of FL caspase-7 remaining in (B and D) upon cleavage by caspase-9 (C) or caspase-8 (E). Values and error bars represent the mean ± SEM for measurements from three independent experiments.

(F) Caspase-7 phosphorylation sites T173 and S30 were replaced by alanine in the background of the C186A substitution of the catalytic cysteine to prevent self-cleavage. Caspase-7 T173A and S30A were treated with PAK2 with or without [γ-^{32}P]ATP, then subjected to cleavage by caspase-9. Caspase-7 T173A/C186A was cleaved faster in the absence of ATP, with rates resembling caspase-7 FL C186A. Caspase-7 S30A/C186A was cleaved at a similar rate in the presence or absence of ATP.

(G and H) Quantification of cleavage in (F) of caspase-7 variants by caspase-9: T173A/C186A (G) or S30A/C186A (H). The nearly identical rate of cleavage of S30A with or without ATP suggests that S30 phosphorylation is responsible for slowing cleavage of caspase-7 FL by caspase-9. Values and error bars represent the mean ± SEM of three independent experiments.

In all parts of this figure, all caspase-7 variants were expressed from a full-length construct that produces residues 1–303 as a single polypeptide chain.

be analyzed. In addition, the large subunit was phosphorylated regardless of the cleavage state of PAK2 (Figures 2A–2C). Despite the overwhelmingly fast phosphorylation by PAK2 in the large subunit, no effect on the catalytic rate of cleaved caspase-7 was observed (Figure S4).

To determine if this phosphorylation occurred at the reported sites on the large subunit, S30 and T173 were individually replaced by alanine, a non-phosphorylatable residue. These substitutions were made in the background of caspase-7 catalytic site inactivation (C186A), which was used to prevent PAK2 from being cleaved. PAK2 did not phosphorylate S30A/C186A but did phosphorylate C186A and T173A/C186A. This was true for both full-length and cleaved caspase-7, indicating that S30 is the primary phosphorylation site on the caspase-7 large subunit (Figure 4A). The ratios of the band intensities for the ^{32}P:Coomassie-stained

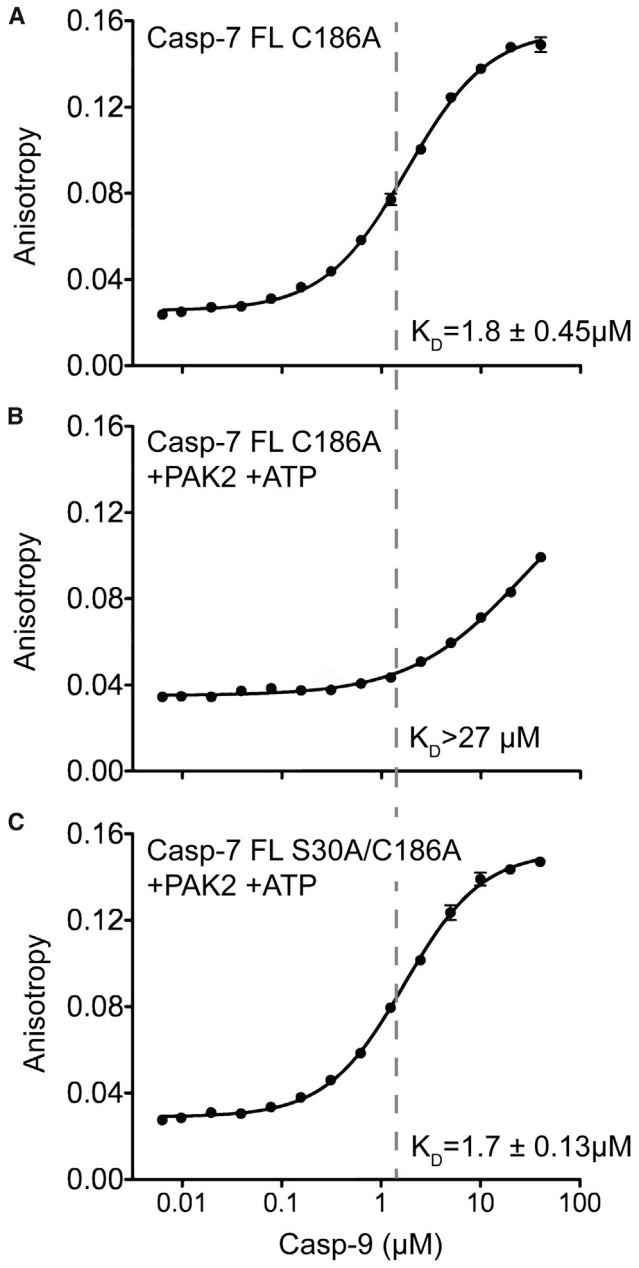

Figure 5. The Interaction between Caspase-7 and Caspase-9 Is Disrupted by Phosphorylation at S30

(A) Fluorescently labeled uncleaved caspase-7 FL C186A interacts by fluorescence polarization with caspase-9 constitutive dimer (cDimer) C287A.

(B) Phosphorylating caspase-7 FL C186A prior to a caspase-9 titration dramatically affects the K_D.

(C) Replacing S30 with a non-phosphorylatable residue (alanine) abrogates phosphorylation by PAK2, enabling a caspase-7:caspase-9 interaction.

Values and error bars represent the mean ± SEM of duplicate measurements taken on each of three separate days.

bands were similar for FL C186A (2.14) and cleaved C186A (2.17) as well as for FL T173A/C186A (2.17) and cleaved T173A/C186A (2.11), suggesting that phosphorylation at S30A occurs similarly on the zymogen and the cleaved forms of caspase-7.

Phosphorylation of Caspase-7 Diminishes Processing by Initiator Caspases

Given that S239 phosphorylation directly affects catalytic activity, it was surprising that the predominant site of phosphorylation, S30, had no direct effect on caspase-7 catalytic function. This suggested that S30 phosphorylation might play an orthogonal functional role. Executioner caspases including caspase-7 are dependent on activation by upstream initiator caspases, including caspase-8 and -9, which cleave the intersubunit linker of full-length procaspase-7 at D198 or D206, generating active caspase-7. To determine if phosphorylation of the full-length caspase-7 affected processing by initiator caspases, full-length caspase-7 C186A was phosphorylated by autoactivated PAK2 in the presence of [γ-^{32}P]ATP or not phosphorylated in the no ATP condition. Phosphorylation was confirmed by autoradiography. Phosphorylated or unphosphorylated caspase-7 was then subjected to cleavage by either caspase-9 or caspase-8. Unphosphorylated caspase-7 was cleaved by caspase-9 completely at the intersubunit linker after 3 hr (Figure 4B). In contrast, phosphorylated caspase-7 was cleaved more slowly by caspase-9. Remaining full-length caspase-7 was quantified at each time point. We observed a significant decrease in the rate of cleavage when caspase-7 was phosphorylated (Figure 4C). Phosphorylated caspase-7 was also cleaved more slowly by caspase-8 (Figures 4D and 4E). For both initiator caspases, 30% less full-length caspase-7 was cleaved in the time course of the experiment. Notably, PAK2 has no effect on the function of either caspase-8 or caspase-9 under these assay conditions (Figures S5A and S5B) and does not phosphorylate caspase-9 at all (Figure S5C), indicating that the decrease in processing is the result of phosphorylation of caspase-7.

Phosphorylation at S30 Slows Processing of Caspase-7 at the Intersubunit Linker

By substituting alanine, a non-phosphorylatable residue, at each of the reported PAK2 sites in the caspase-7 large subunit (T173 and S30), we interrogated the contribution of phosphorylation at these sites to cleavage by caspase-9 (Figure 4F). Caspase-7 T173A/C186A was incubated with PAK2 in the presence or absence of [γ-^{32}P]ATP and subsequently treated with active caspase-9 (Figures 4F and 4G). The cleavage pattern was nearly identical to caspase-7 C186A (Figure 4B), suggesting that phosphorylation at T173 plays no role in slowing cleavage by caspase-9 at the intersubunit linker. In contrast, the cleavage pattern for full-length caspase-7 S30A/C186A was identical in the presence or absence of phosphorylation (Figures 4F and 4H). These data strongly suggest that phosphorylation by PAK2 at S30 has considerable impact on the ability of caspase-9 to cleave caspase-7 at the intersubunit linker (residues 198–206).

Phosphorylation at S30 Interrupts the Binding Interaction between Caspase-7 and Caspase-9

S30 and the cleavage sites in the intersubunit linker (D198/D206) are distal in sequence, and due to the disorder in all structures of the caspase-7 prodomain, it is difficult to draw specific conclusions about the spatial proximity of these two regions. Nevertheless, phosphorylation at caspase-7 S30 clearly affects the ability of caspase-9 to cleave caspase-7 at the intersubunit

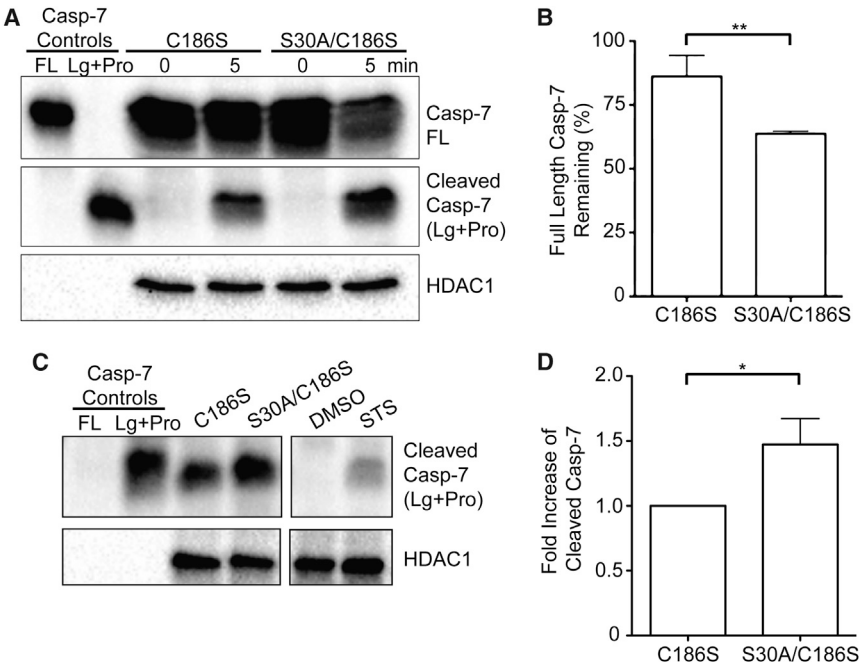

Figure 6. S30 Phosphorylation Regulates Caspase-7 Processing Intracellularly

(A) Caspase-7 FL C186S or S30A/C186S were transiently transfected into MCF7 cells. Activated caspase-9 cleaved caspase-7 FL S30A/C186S faster than C186S in MCF7 lysates. Caspase-7 and histone deacetylase-1 (HDAC-1; a loading control) were observed by immunoblotting.

(B) The band intensity of the remaining FL caspase-7 transfected variants was quantified and normalized to the HDAC-1 loading control. The non-phosphorylatable caspase-7 variant S30A was cleaved faster by caspase-9 than by caspase-7 containing native phosphorylatable S30. Data are shown as means ± SD from experiments performed on three separate days; the asterisks indicate a statistically significant increase in cleavage (**$p < 0.01$) as determined by Student's t test.

(C) Caspase-7 FL C186S or caspase-7 FL S30A/C186S was transiently transfected into MCF7 cells and treated with two compounds known to activate caspase-9 via the intrinsic apoptotic pathway (ABT-263 and A1210477). Cells undergoing apoptosis cleaved caspase-7 FL S30A/C186S faster than C186S. Caspase-7 and histone deacetylase-1 (HDAC-1; a loading control) were monitored by immunoblotting.

(D) The band intensity of the appearance of cleaved caspase-7 was quantified and normalized to the HDAC-1 loading control. The non-phosphorylatable S30A/C186S variant was cleaved approximately 1.4-fold faster than the C186S counterpart. Data are shown as means ± SD from experiments performed on three separate days; the asterisks indicate a statistically significant increase in cleavage (*$p < 0.05$) as determined by Student's t test.

linker. Fluorescence polarization of fluorescein isothiocyanate (FITC)-labeled caspase-7 in the presence of an engineered caspase-9, which forms constitutive dimer (Chao et al., 2005), showed a strong (1.8 μM) interaction (Figures 5A and S6A–S6C). In these experiments, catalytically inactive caspase-7 and -9 were used to prevent cleavage of either caspase during the reaction. When FITC-caspase-7 C186A was incubated with autoactivated PAK2 to allow phosphorylation prior to the caspase-9 titration, the K_D weakened substantially to greater than 27 μM (Figure 5B). This suggests that phosphorylation at S30 blocks the caspase-7:caspase-9 interaction. Consistent with that interpretation, repeating the experiment with caspase-7 S30A/C186A, which is non-phosphorylatable at position 30, shows a similarly strong interaction (K_D = 1.7 μM, Figure 5C) even in the presence of active PAK2. These data confirm the observation (Figures 4C and 4H) that phosphorylation at S30 has a profound effect on how the initiator caspase-9 interacts with the executioner caspase-7 at the initiation stage of apoptosis and may suggest that the N-terminal region of caspase-7 is critical for direct binding to caspase-9.

Non-phosphorylatable Caspase-7 Is Cleaved Faster by Caspase-9 Intracellularly

It is clear that in vitro, phosphorylation at S30 leads to slower cleavage of caspase-7 by caspase-9 at the intersubunit linker. To observe the impact of S30 phosphorylation in a biological context, we used MCF7 cells, a widely used breast cancer model. MCF7 cells are intrinsically deficient in caspase-3, putting the burden of executioner apoptotic activity on caspase-7. In addition, MCF7 cells overexpress PAK2, which phosphorylates caspase-7 intracellularly. MCF7 cells were transiently transfected with either phosphorylatable or non-phosphorylatable (S30A) caspase-7. Both transfected variants carried the catalytically inactivating C186S substitution to prevent caspase-7 self-processing. As predicted, following transfection of MCF7 cells, non-phosphorylatable caspase-7 (S30A/C186S) was processed by added caspase-9 significantly faster than was phosphorylatable caspase-7 (C186S) (Figures 6A and 6B).

After observing the inhibitory effects of phosphorylation of caspase-7 at S30 in the MCF7 cellular milieu, we hypothesized that we would observe a similar effect in growing cells. MCF7 cells transiently transfected with caspase-7 C186S or S30A/C186S were treated with both ABT-263, a Bcl-2 inhibitor, and A1210477, an Mcl2 antagonist, which together stimulate the intrinsic apoptotic pathway and activate caspase-9 (Leverson et al., 2015). Monitoring the appearance of the cleaved and activated caspase-7 (Figures 6C and 6D) revealed that caspase-7 S30A/C186S was processed from the full-length form to the cleaved form faster than the C186S variant. This suggests that, as was the case in vitro, when S30 is available for phosphorylation by PAK2, this site becomes phosphorylated, decreasing binding, recognition, and cleavage by caspase-9. Thus, it becomes clear that PAK2 regulates caspase-7 activity by inhibiting active (cleaved) caspase-7 through phosphorylation at S239, as well as preventing or dramatically slowing caspase-7 activation by caspase-9 due to phosphorylation at S30.

DISCUSSION

The regulation of caspases is paramount for determining whether cells live or die. Global regulation of apoptotic caspases has proven to be heavily modulated by phosphorylation, with

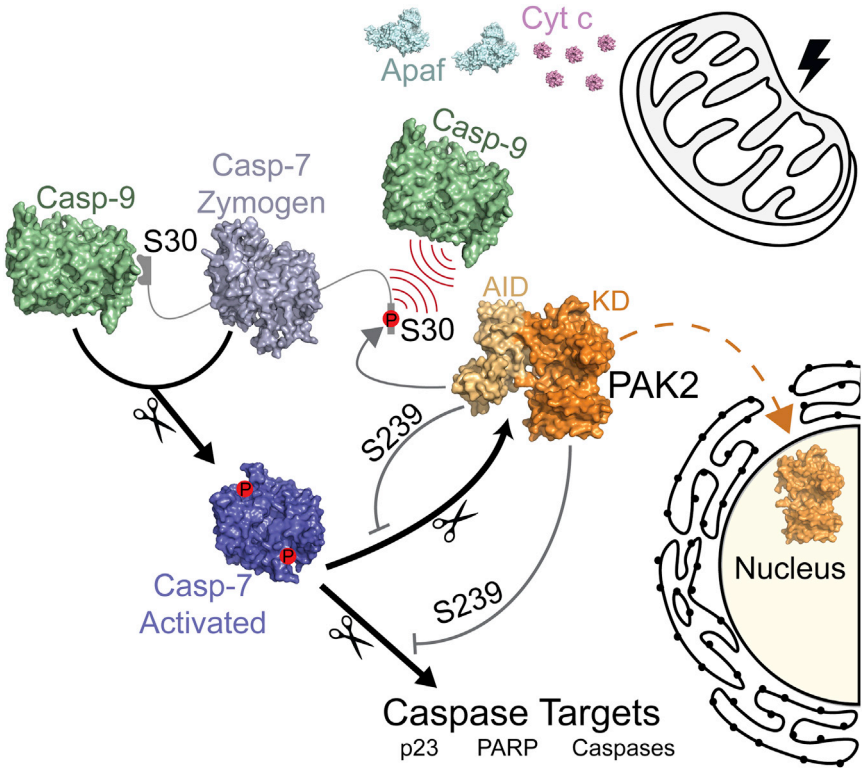

Figure 7. PAK2 Uses Distinct Mechanisms at Two Sites of Phosphorylation: S30 Blocks Caspase-7 Zymogen Activation while S239 Directly Disrupts Substrate Cleavage

The intrinsic apoptotic cascade proceeds when intracellular stresses promote release of cytochrome *c* from the mitochondria. Cytochrome *c* and Apaf-1 constitute the apotosome, which recruits and activates initiator caspase-9. Activated caspase-9 binds the full-length procaspase-7 zymogen, likely through interactions with the N-terminal region containing S30. Caspase-9 activates caspase-7 through cleavage at the intersubunit linker. Active caspase-7 continues the execution of apoptosis by processing over 100 downstream substrates, including p23, PARP, and other caspases. In addition, cleavage of PAK2 by caspases results in a release of the autoinhibitory domain (AID) and signals the kinase domain (KD) to be transported to the nucleus where phosphorylation of new targets propagates the apoptotic response. When active, full-length PAK2 can supersede cell death by performing either of two distinct phosphorylation events on caspase-7. Phosphorylation (℗) at S30 interrupts the interaction between caspase-9 with the caspase-7 zymogen (repelling red lines), thus slowing zymogen activation at the early stages of apoptosis. PAK2 phosphorylation on active caspase-7 at S239 occurs most rapidly when the active-site loops adopt a zymogen-like conformation but abolishes activity in all forms of caspase-7 by directly blocking substrate binding.

extensive phosphorylation on both initiator and executioner caspases typically leading to inactivation (for review see Kurokawa and Kornbluth, 2009; López-Otín and Hunter, 2010). Prior to this work, the molecular details of these inactivating events have been sparse. Emerging regulatory themes have demonstrated an intricate complexity, with caspases as kinase substrates and kinases as caspase substrates. Biases in this interplay that favor cell survival influence diseases of proliferation, like cancer. In the caspase-7:kinase co-regulation, PAK2 hyperactivity is observed to contribute to a cancerous phenotype, with enhanced cell survival and chemotherapeutic resistance (Li et al., 2011).

Our results mechanistically highlight the functional relevance of PAK2 directly phosphorylating the apoptotic target caspase-7 and demonstrate how PAK2 affects caspase-7 activity independently prior to (S30 phosphorylation) or after (S239 phosphorylation) caspase-7 activation in apoptosis. The first mechanism slows initial activation by allosterically disrupting the ability of initiator caspases to activate full-length procaspase-7 prior to apoptosis, while the second mechanism involves direct blocking of substrate from binding to active caspase-7 during apoptosis (Figure 7).

Phosphorylation at S30 interrupts the binding interaction of caspase-7 with the initiator, caspase-9, and thereby slows caspase-7 cleavage at the distal intersubunit linker. Phosphorylation has been observed to directly block cleavage at the intersubunit linker of several caspases, including caspase-2 (Shin et al., 2005), caspase-3 (Duncan et al., 2011), caspase-8 (Cursi et al., 2006; Matthess et al., 2010), and murine caspase-9 (McDonnell et al., 2008). A recent study identified a phosphorylation site distal from the intersubunit linker cleavage site that decreases caspase-8 processing through the sequential action of two kinases via an as yet unknown mechanism (Matthess et al., 2014). Phosphorylation of S30 of caspase-7 is the first report of direct allosteric regulation of zymogen activation in caspases, where phosphorylation at a distal site affected intersubunit linker cleavage. In many previous cases, the phosphorylation sites that affect the rate of activation were located either on the linker itself or directly adjacent in the immediate flanking sequence, suggesting that phosphorylation at those linker sites directly prevents binding of the activating caspase by introduction of a charged residue. Inhibition by phosphorylation at S30 is the first example revealing details of a one-step allosteric mechanism where a distant site is utilized to control caspase maturation from the zymogen to the active form. We know of no other proteases for which this mechanism of phosphorylation regulating zymogen activation by a single kinase has been reported, but one might speculate that zymogen activation of other caspases or other proteases may likewise be allosterically modulated by relevant kinases. This identification of a vulnerable allosteric site on caspase-7 opens the door for future modulation of caspase-7 activation by both caspase and kinase modulators.

S30 sits in the N-terminal region of caspase-7. Our data suggest that this region may be critical for directly mediating the interaction of caspase-7 with caspase-9, potentially through an exosite interaction, that leads to zymogen activation. This N-terminal region has never been structurally characterized as it has been disordered in the many structures of caspase-7. Nevertheless, this region has proven to be critical for the participation of

caspase-7 in apoptosis using allosteric mechanisms. An exosite at a basic lysine patch (K^{38}KKK) assists in the recognition of specific caspase-7 substrates (Boucher et al., 2012). While little is known about the region, it appears to be critical for caspase-7 specific activities. For example, the K^{38}KKK is not present in caspase-3 and is one example of how caspase-7 is able to fulfill its non-redundant apoptotic roles during the demolition phase. The PAK2 motif containing S30 is not present in caspase-3. We have also observed that PAK2 does not phosphorylate caspase-3 in this N-terminal region in vitro (data not shown), which further suggests that this region of caspase-7 is a region that is critical for regulation of caspase-7 specifically.

While phosphorylation of caspase substrates has been observed to block their cleavage by caspases, our work is the first to show that phosphorylation of an active-site loop in a caspase directly blocks substrate binding, thus inactivating active caspase-7 and later during apoptosis. The crystal structure of caspase-7 phosphomimetic S239E suggests that steric bulk and charge from phosphorylation result in a misalignment of the active-site loop 3. This mechanism is similar to that observed for caspase-6 phosphorylation of S257 by Ark5 kinase, which leads to misalignment of the loops in the substrate-binding groove and inactivation of caspase-6 (Velázquez-Delgado and Hardy, 2012). Many lines of evidence have suggested that active-site loop conformations are critical for caspase function. Cleavage of the intersubunit linkers liberates two loops, which can reorganize to facilitate substrate binding. Mechanisms like those utilized by PAK2 and Ark5 take advantage of the requirement for precise positioning of the loops to enable substrate binding and cleavage. Small molecules and mutations that organize (Walters et al., 2009) or disorganize (Hardy and Wells, 2009; Hardy et al., 2004) the active-site loops have proven to be effective activators or inhibitors. The discovery of the dimer interface allosteric site in caspases led to speculation that a naturally occurring regulatory small molecule might bind and inactivate caspase-7. Our observation that S239 becomes accessible upon binding small molecules at this allosteric site (containing C290) may suggest that such a molecule would be synergistic with PAK2, enabling phosphorylation at S239, thereby inhibiting caspase-7 activity in a covalent, and perhaps more stable, manner. Future caspase therapeutics may fruitfully focus on this adaptable regulatory mechanism exploited by PAK2.

Together, phosphorylation of PAK2 at both S30 and S239 combine to exert powerful control over the activation and subsequent activity of caspase-7. The effects of phosphorylation are maximized by taking advantage of a dual mechanism: an initial phosphorylation at S30 is responsible for slowing the critical activation event of intersubunit linker cleavage followed by a second modification on S239 to disrupt the active-site loops and directly block substrate binding (Figure 7). This phenomenon, wherein one kinase engages two different molecular mechanisms that each lead to the same overall cellular outcome, has been observed for other kinase-substrate pairs. Ribosomal protein S6 kinase β-1 (S6K1) phosphorylation of insulin receptor substrate 1 (IRS-1) at S1101 blocks its interaction with phosphatidylinositol 3-kinase, leading to insulin resistance (Tremblay et al., 2007). When alternative IRS-1 sites, S307/S312, are phosphorylated by S6K1, it enhances proteasomal degradation, also leading to insulin resistance (Greene et al., 2003; Shah and Hunter, 2006). This pattern of regulation can also be observed for transcriptional regulation by the forkhead box proteins (FOXO). FOXO1 is phosphorylated by protein kinase B (PKB/Akt) at three sites, T24, S256, and S319 (Rena et al., 1999), which results in a loss of transcriptional activity. Similar to PAK2 regulation of caspase-7, PKB phosphorylation utilizes different mechanisms of inhibition to achieve the same overall biological goal. Phosphorylation at S256 limits FOXO1 DNA binding (Zhang et al., 2002). Meanwhile, phosphorylation at S319 creates a consensus sequence for CK1 to phosphorylate additional serine residues at positions 322 and 325 (Rena, 2002). This tight grouping of modified serines promotes the nuclear export of FOXO1, decreasing FOXO1 activity by a different mechanism. In these patterns of regulation, one kinase modifies a single substrate at multiple sites, which each exert mechanistically independent but biologically synergistic effects. This synergy in impact is perhaps expected, as uncorrelated outcomes would be nonproductive. Thus, it is likely that full-length PAK2 would only play anti-apoptotic roles that have biological synergy to caspase-7 phosphorylation under related conditions.

In addition to S30 and S239, T173 has also been reported to be phosphorylated by PAK2 (Li et al., 2011). We have not observed phosphorylation of T173 under any conditions, nor have we observed any functional effect of phosphomimetics at this residue. This could be because (1) we have not explored the requisite conditions for phosphorylation, or (2) T173 is not a bona fide modification site but can only be recognized in a peptide, such as those used to identify this site (Li et al., 2011), not in an intact protein, or (3) T173 is a bystander residue, which has no functional effect upon phosphorylation. The concept of bystander residues is replete in the kinase literature. Our work on S30 demonstrates that, even for functional phosphorylation events, it can be difficult to decipher the role that phosphorylation at a given site might play. It is possible that we may not have found the right conditions for T173 phosphorylation by PAK2, but if T173 is a target of PAK2 under conditions where S30 and S239 are phosphorylated it should likewise have an anti-apoptotic effect. We may likewise predict that if phosphorylation of T173 by PAK2 has a different (e.g., pro-apoptotic) functional effect, we would expect to observe it only under very different cellular conditions. In addition, it is possible that each of the three sites of phosphorylation are utilized under different biological conditions, providing nuanced control of caspase-7 activity by PAK2.

These findings illuminate the molecular details of a kinase inhibiting an apoptotic caspase. The implications extend to cancer resistance, suggesting a hyperactive PAK2 is able to limit apoptotic cell death and resist apoptotic stimulation by chemotherapeutic agents. In addition, our results pinpoint an allosteric region on a key apoptotic contributor, where alterations result in a slowed maturation and potential control over an executioner caspase. The significance of this regulation could extend beyond cancer resistance and apoptotic activation. Recent discoveries have implicated caspase-7 in inflammation (Erener et al., 2012; Lamkanfi et al., 2008), defense against *Legionella pneumophila* infection (Akhter et al., 2009), osteogenesis (Svandova et al., 2014), and tooth development (Matalova et al., 2013), all of which show that caspase-7 has distinct roles from caspase-3. These non-apoptotic roles could share regulation by phosphorylation and the mechanistic details uncovered here.

Finally, our increased mechanistic understanding of details of this caspase:kinase interplay may guide precision therapeutic approaches that exploit synergies between caspase- and kinase-directed modulators. Likewise, identification of the S30 site as critical for interaction with caspase-9 may implicate this S30 region in playing a role in the recognition of other caspase-7 substrates. If this is the case, synthetic inhibitors that block the S30 region, mimicking S30 phosphorylation, may prevent cleavage of the subset of substrates that utilize the S30 region for binding. This is in contrast to active-site-directed inhibitors, which like S239 phosphorylation, block cleavage of all caspase-7 substrates. S30-mimicking inhibitors that offered precision control of substrate selection would be unprecedented in the realm of synthetic caspase regulation.

EXPERIMENTAL PROCEDURES

Generation of Caspase-9 Constitutive Dimer

Caspase-9 exists primarily as a monomer in solution, as seen by size-exclusion chromatography (Huber and Hardy, 2012). A constitutively dimeric caspase-9 has been reported, which decreases the distribution of caspase-9 monomers in solution and increases the more biologically relevant dimer (Chao et al., 2005). In this dimeric caspase-9, five residues at the dimer interface of caspase-9 were replaced with the residues from caspase-3. We followed this strategy and replaced the codons for residues 402–406 to the caspase-3 equivalent C-I-V-S-M on the C terminus of caspase-9 C287A using Phusion site-directed mutagenesis (Thermo Scientific).

In Vitro Phosphorylation Assays

Purified recombinant PAK2 T402E was first allowed to auto-activate by incubation with 1 mM ATP in PAK2 activity buffer (50 mM Tris [pH 7.5], 20 mM $MgCl_2$, 0.1 mM EDTA, 2 mM DTT) for 1 hr at 30°C. This activated kinase was then incubated with caspase-7 variants at a 20:1 caspase:kinase ratio. In addition, [γ-^{32}P]ATP (10 μCi/μL) was added to radioactively label phosphorylation on the caspase subunits. Reactions were resolved by SDS-PAGE and visualized by autoradiography using a Typhoon FLA 7000 (GE Healthcare). Band quantification was carried out by ImageQuant software (GE Healthcare) using a set of [γ-^{32}P]ATP standards.

PAK2 is also a substrate of caspase-7, and under certain conditions caspase-7 will cleave PAK2. In order to silence this enzymatic activity, but still run the in vitro phosphorylation assay, active forms of caspase-7 could be silenced by incubation with a PG (L-cysteinyl-2-pyridyl disulfide) (Ventura et al., 2015) that targets free activated cysteines on the caspase. Prior to the in vitro phosphorylation assay, 20 μM caspase-7 was incubated with 2 mM PG for 1 hr in 20 mM Tris (pH 7.5), 100 mM NaCl, and was buffer exchanged to reduce the concentration of reductant (DTT) remaining after purification. This inactive caspase-7 was then used in an identical fashion to the in vitro phosphorylation assay described above.

Caspase Cleavage Assays

To monitor the impact of caspase-7 phosphorylation on cleavage of full-length caspase-7 by the initiators caspase-8 or -9, caspase-7 zymogen was first incubated with PAK2. In this experiment, all of the caspase-7 variants had the catalytic cysteine mutated to alanine (C186A) in order to ensure that all observed cleavage was from the initiator caspases. Caspase-7 full-length C186A and phospho-knockouts (S30A, T173A) were first incubated with pre-activated PAK2 (as described above) or with PAK2 in the absence of ATP, in PAK2 activity buffer for 3 hr at 30°C. In addition, [γ-^{32}P]ATP (10 μCi/μL) was added to radioactively label phosphorylation on the caspase subunits. The equivalent volume of water was added to each reaction in the "no ATP" controls. Treated caspase-7 was then diluted to 3 μM in caspase-9 activity assay buffer (100 mM MES [pH 6.5], 20% PEG 400, and 5 mM DTT) or in caspase-8 activity assay buffer (10 mM PIPES [pH 7.2], 0.1 M NaCl, 1 mM EDTA, 10% sucrose, 0.05% CHAPS, and 5 mM DTT). The corresponding initiator caspase was added at a final concentration of 500 nM. The reaction was quenched at each time point by the addition of SDS sample buffer and boiled for 10 min. Cleavage was assessed by SDS-PAGE analysis, and band quantification was determined using Image Lab software (Bio-Rad).

Fluorescence Anisotropy

Fluorescence anisotropy was monitored using a SpectraMax M5 plate reader (Molecular Devices) with a fixed excitation wavelength set to 485 nm and an emission wavelength set to 525 nm. Full-length caspase-7 C186A or full-length caspase-7 S30A/C186A was labeled with FITC isomer 1 (Sigma) in 0.1 M sodium bicarbonate buffer at pH 9.0. After labeling, unreacted FITC was removed from labeled caspase-7 by buffer exchanging with 3K molecular weight cutoff filters into 100 mM Tris (pH 7.5) and 100 mM NaCl. A fixed concentration of 20 nM labeled protein was subjected to serial dilution of caspase-9 constitutive dimer C287A from 40 μM to 10 nM. All measurements were taken at 25°C after a 1 hr incubation.

MCF7 Lysate Cleavage Assay

MCF cells were first washed twice with ice-cold 1× PBS and then lysed in 50 mM Tris (pH 7.4), 150 mM NaCl, 1% Triton X-100, and protease inhibitors (1 mM 4-(2-aminoethyl)benzenesulfonyl fluoride, 0.8 μM aprotinin, 29 μM bestatin, 10 μM pepstatin, and 1.3 mM EDTA) and phosphatase inhibitors (5 mM β-glycerophosphate, 20 mM sodium fluoride, and 200 μM sodium orthovanadate) on ice for 30 min, and then centrifuged at 20,000 relative centrifugal force for 20 min at 4°C. Quantification of total protein levels in the supernatant were determined using the bicinchoninic acid assay (Pierce). An equal amount of total protein was then subjected to caspase-9 cleavage by the addition of 0.93 μg/μL of purified recombinant human caspase-9.

MCF7 Whole-Cell Caspase-7 Cleavage Assay

MCF7 cells were grown to ~90% confluency and then plated in six-well plates with one million cells per well. Cells were transiently transfected with caspase-7 C186S DNA or caspase-7 S30A/C186S DNA using Lipofectamine 3000 (Invitrogen) according to the manufacturer's instructions. Cells were then treated with DMSO, staurosporine (1 μM), or apoptosis-inducing compounds (ABT-263 and A1210477; 10 μM) for 3 hr. After incubation with compounds, cells were trypsinized and washed twice with ice-cold 1× PBS buffer. Cells were then lysed as described previously and lysates were quantified using the bicinchoninic acid assay (Pierce). An equal amount of total protein was loaded into each well of a 12% acrylamide gel and cleaved caspase-7 was detected by western blot analysis. The protocol for immunoblotting is given in the Supplemental Experimental Procedures.

Additional Experimental Procedures

DNA expression constructs, antibodies, expression, purification, mutagenesis and activity assay protocols for caspase-7, -8, and -9 and PAK2, crystallization, structure determination, immunoblotting, cell culture, and transfection can be found in the Supplemental Experimental Procedures.

ACCESSION NUMBERS

The accession number for the coordinates and structure factors reported in this paper is PDB: 5K20.

SUPPLEMENTAL INFORMATION

Supplemental Information includes Supplemental Experimental Procedures, six figures, and one table and can be found with this article online at http://dx.doi.org/10.1016/j.str.2016.11.001.

AUTHOR CONTRIBUTIONS

S.J.E. initiated and performed all experimental aspects of the study, prepared all figures and was the principal author for the manuscript. K.R. synthesized the cysteinyl-2-pyridyl disulfide protecting group. J.A.H. conceptualized the project, secured funding, directed the research project, wrote parts of the manuscript and edited the manuscript.

ACKNOWLEDGMENTS

This work was supported by the NIH (GM80532). We thank V. Stojanoff and E. Lazo for assistance with data collection and acknowledge NSLS X6A, which is funded by the National Institute of Health (GM-0080), and the National Synchrotron Light Source at Brookhaven National Laboratory, which is supported by the U.S. Department of Energy (DE-AC02-98CH10886). We thank S. Thayumanavan for providing support to K.R. for synthesis of the cysteinyl-2-pyridyl disulfide.

Received: June 27, 2016
Revised: September 20, 2016
Accepted: October 27, 2016
Published: November 23, 2016

REFERENCES

Agard, N.J., Mahrus, S., Trinidad, J.C., Lynn, A., Burlingame, A.L., and Wells, J.A. (2012). Global kinetic analysis of proteolysis via quantitative targeted proteomics. Proc. Natl. Acad. Sci. USA *109*, 1913–1918.

Akhter, A., Gavrilin, M.A., Frantz, L., Washington, S., Ditty, C., Limoli, D., Day, C., Sarkar, A., Newland, C., Butchar, J., et al. (2009). Caspase-7 activation by the Nlrc4/Ipaf inflammasome restricts *Legionella pneumophila* infection. PLoS Pathog. *5*, e1000361.

Allan, L.A., and Clarke, P.R. (2007). Phosphorylation of caspase-9 by CDK1/Cyclin B1 protects mitotic cells against apoptosis. Mol. Cell *26*, 301–310.

Allan, L.A., Morrice, N., Brady, S., Magee, G., Pathak, S., and Clarke, P.R. (2003). Inhibition of caspase-9 through phosphorylation at Thr 125 by ERK MAPK. Nat. Cell Biol. *5*, 647–654.

Alvarado-Kristensson, M., Melander, F., Leandersson, K., Rönnstrand, L., Wernstedt, C., and Andersson, T. (2004). p38-MAPK signals survival by phosphorylation of caspase-8 and caspase-3 in human neutrophils. J. Exp. Med. *199*, 449–458.

Andersen, J.L., Johnson, C.E., Freel, C.D., Parrish, A.B., Day, J.L., Buchakjian, M.R., Nutt, L.K., Thompson, J.W., Moseley, M.A., and Kornbluth, S. (2009). Restraint of apoptosis during mitosis through interdomain phosphorylation of caspase-2. EMBO J. *28*, 3216–3227.

Boucher, D., Blais, V., and Denault, J.-B. (2012). Caspase-7 uses an exosite to promote poly(ADP ribose) polymerase 1 proteolysis. Proc. Natl. Acad. Sci. USA *109*, 4–9.

Cardone, M.H., Roy, N., Stennicke, H.R., Salvesen, G.S., Franke, T.F., Stanbridge, E., Frisch, S., and Reed, J.C. (1998). Regulation of cell death protease Caspase-9 by phosphorylation. Science *282*, 1318–1321.

Chao, Y., Shiozaki, E.N., Srinivasula, S.M., Rigotti, D.J., Fairman, R., and Shi, Y. (2005). Engineering a dimeric caspase-9: a re-evaluation of the induced proximity model for caspase activation. PLoS Biol. *3*, 1079–1087.

Cursi, S., Rufini, A., Stagni, V., Condò, I., Matafora, V., Bachi, A., Bonifazi, A.P., Coppola, L., Superti-Furga, G., Testi, R., et al. (2006). Src kinase phosphorylates Caspase-8 on Tyr380: a novel mechanism of apoptosis suppression. EMBO J. *25*, 1895–1905.

Dagbay, K., Eron, S.J., Serrano, B.P., Velázquez-Delgado, E.M., Zhao, Y., Lin, D., Vaidya, S., and Hardy, J.A. (2014). A multipronged approach for compiling a global map of allosteric regulation in the apoptotic caspases. Methods Enzymol. *544*, 215–249.

Dhillon, A.S., Hagan, S., Rath, O., and Kolch, W. (2007). MAP kinase signalling pathways in cancer. Oncogene *26*, 3279–3290.

Dix, M.M., Simon, G.M., and Cravatt, B.F. (2008). Global mapping of the topography and magnitude of proteolytic events in apoptosis. Cell *134*, 679–691.

Dix, M.M., Simon, G.M., Wang, C., Okerberg, E., Patricelli, M.P., and Cravatt, B.F. (2012). Functional interplay between caspase cleavage and phosphorylation sculpts the apoptotic proteome. Cell *150*, 426–440.

Dummler, B., Ohshiro, K., Kumar, R., and Field, J. (2009). Pak protein kinases and their role in cancer. Cancer Metastasis Rev. *28*, 51–63.

Duncan, J.S., Turowec, J.P., Duncan, K.E., Vilk, G., Wu, C., Luscher, B., Li, S.S.-C., Gloor, G.B., and Litchfield, D.W. (2011). A peptide-based target screen implicates the protein kinase CK2 in the global regulation of caspase signaling. Sci. Signal. *4*, ra30.

Erener, S., Pétrilli, V., Kassner, I., Minotti, R., Castillo, R., Santoro, R., Hassa, P.O., Tschopp, J., and Hottiger, M.O. (2012). Inflammasome-activated Caspase 7 cleaves PARP1 to enhance the expression of a subset of NF-κB target genes. Mol. Cell *46*, 200–211.

Ghavami, S., Shojaei, S., Yeganeh, B., Ande, S.R., Jangamreddy, J.R., Mehrpour, M., Christoffersson, J., Chaabane, W., Rezaei, A., Kashani, H.H., et al. (2014). Autophagy and apoptosis dysfunction in neurodegenerative disorders. Prog. Neurobiol. *112*, 24–49.

Greenblatt, M.S., Bennett, W.P., Hollstein, M., and Harris, C.C. (1994). Mutations in the p53 tumor suppressor gene: clues to cancer etiology and molecular pathogenesis. Cancer Res. *54*, 4855–4878.

Greene, M.W., Sakaue, H., Wang, L., Alessi, D.R., and Roth, R.A. (2003). Modulation of insulin-stimulated degradation of human insulin receptor substrate-1 by serine 312 phosphorylation. J. Biol. Chem. *278*, 8199–8211.

Hardy, J.A., and Wells, J.A. (2009). Dissecting an allosteric switch in caspase-7 using chemical and mutational probes. J. Biol. Chem. *284*, 26063–26069.

Hardy, J.A., Lam, J., Nguyen, J.T., O'Brien, T., and Wells, J.A. (2004). Discovery of an allosteric site in the caspases. Proc. Natl. Acad. Sci. USA *101*, 12461–12466.

Hill, M.E., MacPherson, D.J., Wu, P., Julien, O., Wells, J.A., and Hardy, J.A. (2016). Reprogramming Caspase-7 specificity by regio-specific mutations and selection provides alternate solutions for substrate recognition. ACS Chem. Biol. *11*, 1603–1612.

Huber, K.L., and Hardy, J.A. (2012). Mechanism of zinc-mediated inhibition of caspase-9. Protein Sci. *21*, 1056–1065.

Jakobi, R., Moertl, E., and Koeppel, M.A. (2001). p21-activated protein kinase gamma-PAK suppresses programmed cell death of BALB3T3 fibroblasts. J. Biol. Chem. *276*, 16624–16634.

Jakobi, R., McCarthy, C.C., Koeppel, M.A., and Stringer, D.K. (2003). Caspase-activated PAK-2 is regulated by subcellular targeting and proteasomal degradation. J. Biol. Chem. *278*, 38675–38685.

Kurokawa, M., and Kornbluth, S. (2009). Caspases and kinases in a death grip. Cell *138*, 838–854.

Lamkanfi, M., Kanneganti, T.-D., Van Damme, P., Vanden Berghe, T., Vanoverberghe, I., Vandekerckhove, J., Vandenabeele, P., Gevaert, K., and Núñez, G. (2008). Targeted peptidecentric proteomics reveals caspase-7 as a substrate of the caspase-1 inflammasomes. Mol. Cell. Proteomics *7*, 2350–2363.

Lee, N., MacDonald, H., Reinhard, C., Halenbeck, R., Roulston, A., Shi, T., and Williams, L.T. (1997). Activation of hPAK65 by caspase cleavage induces some of the morphological and biochemical changes of apoptosis. Proc. Natl. Acad. Sci. USA *94*, 13642–13647.

Leverson, J.D., Zhang, H., Chen, J., Tahir, S.K., Phillips, D.C., Xue, J., Nimmer, P., Jin, S., Smith, M., Xiao, Y., et al. (2015). Potent and selective small-molecule MCL-1 inhibitors demonstrate on-target cancer cell killing activity as single agents and in combination with ABT-263 (navitoclax). Cell Death Dis. *6*, e1590.

Li, X., Wen, W., Liu, K., Zhu, F., Malakhova, M., Peng, C., Li, T., Kim, H.-G., Ma, W., Cho, Y.Y., et al. (2011). Phosphorylation of caspase-7 by p21-activated protein kinase (PAK) 2 inhibits chemotherapeutic drug-induced apoptosis of breast cancer cell lines. J. Biol. Chem. *286*, 22291–22299.

López-Otín, C., and Hunter, T. (2010). The regulatory crosstalk between kinases and proteases in cell cancer. Nat. Rev. Cancer *10*, 278–292.

Margolis, R.L., Chuang, D.M., and Post, R.M. (1994). Programmed cell death: implications for neuropsychiatric disorders. Biol. Psychiatry *35*, 946–956.

Marlin, J.W., Eaton, A., Montano, G.T., Chang, Y.E., and Jakobi, R. (2009). Elevated p21-activated kinase 2 activity results in anchorage-independent growth and resistance to anticancer drug – induced cell death. Neoplasia *11*, 286–297.

Marlin, J.W., Chang, Y.-W.E., Ober, M., Handy, A., Xu, W., and Jakobi, R. (2011). Functional PAK-2 knockout and replacement with a caspase cleavage-deficient mutant in mice reveals differential requirements of full-length PAK-2 and caspase-activated PAK-2p34. Mamm. Genome *22*, 306–317.

Matalova, E., Lesot, H., Svandova, E., Vanden Berghe, T., Sharpe, P.T., Healy, C., Vandenabeele, P., and Tucker, A.S. (2013). Caspase-7 participates in differentiation of cells forming dental hard tissues. Dev. Growth Differ. *55*, 615–621.

Matthess, Y., Raab, M., Sanhaji, M., Lavrik, I.N., and Strebhardt, K. (2010). Cdk1/cyclin B1 controls Fas-mediated apoptosis by regulating caspase-8 activity. Mol. Cell. Biol. *30*, 5726–5740.

Matthess, Y., Raab, M., Knecht, R., Becker, S., and Strebhardt, K. (2014). Sequential Cdk1 and Plk1 phosphorylation of caspase-8 triggers apoptotic cell death during mitosis. Mol. Oncol. *8*, 596–608.

McDonnell, M.A., Abedin, M.J., Melendez, M., Platikanova, T.N., Ecklund, J.R., Ahmed, K., and Kelekar, A. (2008). Phosphorylation of murine caspase-9 by the protein kinase casein kinase 2 regulates its cleavage by Caspase-8. J. Biol. Chem. *283*, 20149–20158.

Mira, J.-P., Benard, V., Groffen, J., Sanders, L.C., and Knaus, U.G. (2000). Endogenous, hyperactive Rac3 controls proliferation of breast cancer cells by a p21-activated kinase-dependent pathway. Proc. Natl. Acad. Sci. USA *97*, 185–189.

Moretti, A., Weig, H.-J., Ott, T., Seyfarth, M., Holthoff, H.-P., Grewe, D., Gillitzer, A., Bott-Flügel, L., Schömig, A., Ungerer, M., et al. (2002). Essential myosin light chain as a target for caspase-3 in failing myocardium. Proc. Natl. Acad. Sci. USA *99*, 11860–11865.

Pistritto, G., Trisciuoglio, D., Ceci, C., Garufi, A., and Orazi, G.D. (2016). Apoptosis as anticancer mechanism: function and dysfunction of its modulators and targeted therapeutic strategies. Aging *8*, 603–619.

Plati, J., Bucur, O., and Khosravi-Far, R. (2010). Dysregulation of apoptotic signaling in cancer: molecular mechanisms and therapeutic opportunities. J. Cell Biochem. *104*, 1124–1149.

Rena, G. (2002). Two novel phosphorylation sites on FKHR that are critical for its nuclear exclusion. EMBO J. *21*, 2263–2271.

Rena, G., Guo, S., Cichy, S.C., Unterman, T.G., and Cohen, P. (1999). Phosphorylation of the transcription factor forkhead family member FKHR by protein kinase B. J. Biol. Chem. *274*, 17179–17183.

Riedl, S.J., Fuentes-Prior, P., Renatus, M., Kairies, N., Krapp, S., Huber, R., Salvesen, G.S., and Bode, W. (2001). Structural basis for the activation of human procaspase-7. Proc. Natl. Acad. Sci. USA *98*, 14790–14795.

Rudel, T., and Bokoch, G.M. (1997). Membrane and morphological changes in apoptotic cells regulated by caspase-mediated activation of PAK2. Science *276*, 1571–1574.

Seaman, J.E., Julien, O., Lee, P.S., Rettenmaeier, T.J., Thomsen, N.D., and Wells, J.A. (2016). Cacidases: caspases can cleave after aspartate, glutamate, and phosphoserine residues. Cell Death Differ. *23*, 1717–1726.

Shah, O.J., and Hunter, T. (2006). Turnover of the active fraction of IRS1 involves raptor-mTOR- and S6K1-dependent serine phosphorylation in cell culture models of tuberous sclerosis. Mol. Cell. Biol. *26*, 6425–6434.

Shin, S., Lee, Y., Kim, W., Ko, H., Choi, H., and Kim, K. (2005). Caspase-2 primes cancer cells for TRAIL-mediated apoptosis by processing procaspase-8. EMBO J. *24*, 3532–3542.

Stennicke, H.R., Renatus, M., Meldal, M., and Salvesen, G.S. (2000). Internally quenched fluorescent peptide substrates disclose the subsite preferences of human caspases 1, 3, 6, 7 and 8. Biochem. J. *350* (Pt 2), 563–568.

Suzuki, A., Kusakai, G.-I., Kishimoto, A., Shimojo, Y., Miyamoto, S., Ogura, T., Ochiai, A., and Esumi, H. (2004). Regulation of caspase-6 and FLIP by the AMPK family member ARK5. Oncogene *23*, 7067–7075.

Svandova, E., Lesot, H., Vanden Berghe, T., Tucker, A.S., Sharpe, P.T., Vandenabeele, P., and Matalova, E. (2014). Non-apoptotic functions of caspase-7 during osteogenesis. Cell Death Dis. *5*, e1366.

Tremblay, F., Brûlé, S., Hee Um, S., Li, Y., Masuda, K., Roden, M., Sun, X.J., Krebs, M., Polakiewicz, R.D., Thomas, G., et al. (2007). Identification of IRS-1 Ser-1101 as a target of S6K1 in nutrient- and obesity-induced insulin resistance. Proc. Natl. Acad. Sci. USA *104*, 14056–14061.

Vaux, D.L., Cory, S., and Adams, J.M. (1988). Bcl-2 gene promotes haemopoietic cell survival and cooperates with c-myc to immortalize pre-B cells. Nature *335*, 440–442.

Velázquez-Delgado, E.M., and Hardy, J.A. (2012). Phosphorylation regulates assembly of the caspase-6 substrate-binding groove. Structure *20*, 742–751.

Ventura, J., Eron, S.J., González-Toro, D.C., Raghupathi, K., Wang, F., Hardy, J.A., and Thayumanavan, S. (2015). Reactive self-assembly of polymers and proteins to reversibly silence a killer protein. Biomacromolecules *16*, 3161–3171.

Walter, B.N., Huang, Z., Jakobi, R., Tuazon, P.T., Alnemri, E.S., Litwack, G., and Traugh, J.A. (1998). Cleavage and activation of p21-activated protein kinase γ-PAK by CPP32 (caspase 3). Effects of autophosphorylation on activity. J. Biol. Chem. *273*, 28733–28739.

Walters, J., Pop, C., Scott, F.L., Drag, M., Swartz, P., Mattos, C., Salvesen, G.S., and Clark, A.C. (2009). A constitutively active and uninhibitable caspase-3 zymogen efficiently induces apoptosis. Biochem. J. *424*, 335–345.

Witkowski, W., and Hardy, J.A. (2009). L2′ loop is critical for caspase-7 active site formation. Protein Sci. *18*, 1459–1468.

Witkowski, W.A., and Hardy, J.A. (2011). A designed redox-controlled caspase. Protein Sci. *20*, 1421–1431.

Worth, A., Thrasher, A.J., and Gaspar, H.B. (2006). Autoimmune lymphoproliferative syndrome: molecular basis of disease and clinical phenotype. Br. J. Haematol. *133*, 124–140.

Zhang, X., Gan, L., Pan, H., Guo, S., He, X., Olson, S.T., Mesecar, A., Adam, S., and Untermant, T.G. (2002). Phosphorylation of serine 256 suppresses transactivation by FKHR (FOXO1) by multiple mechanisms: direct and indirect effects on nuclear/cytoplasmic shuttling and DNA binding. J. Biol. Chem. *277*, 45276–45284.

Zukowski, S.A., and Litchfield, D.W. (2015). Protein kinases and caspases: bidirectional interactions in apoptosis. In Kinomics: Approaches and Applications, H.-B. Kraatz and S. Martic, eds. (Wiley-VCH Verlag), pp. 85–114.

Structure, Volume *25*

Supplemental Information

Dual Site Phosphorylation of Caspase-7 by PAK2 Blocks Apoptotic Activity by Two Distinct Mechanisms

Scott J. Eron, Kishore Raghupathi, and Jeanne A. Hardy

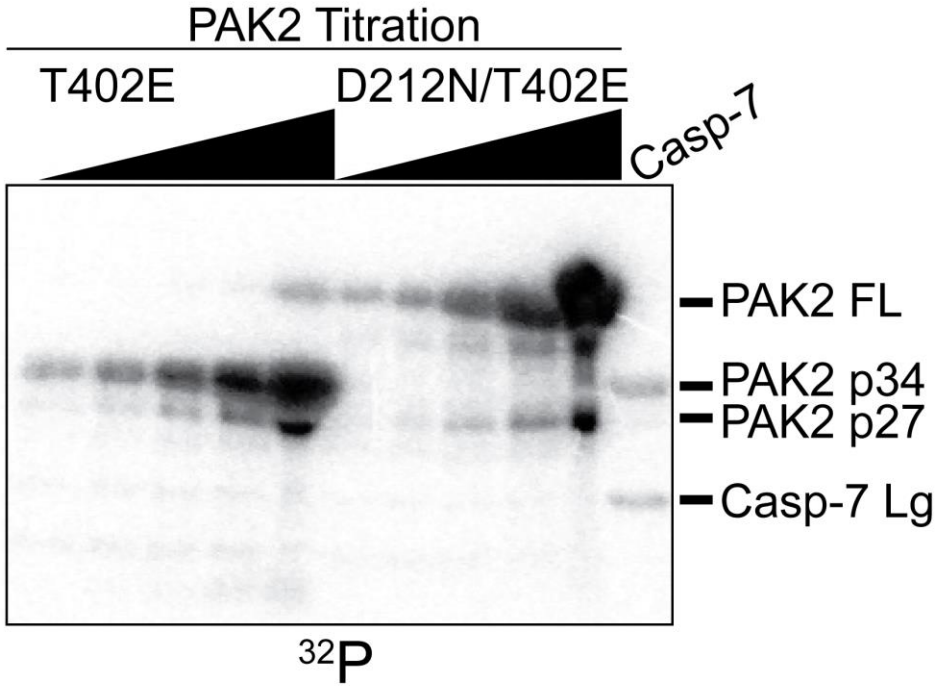

Figure S1: Casp-7 cleaves PAK2 at D212 (Related to Figure 2)
Catalytic amounts of casp-7 CT S30A/T173A were incubated with PAK2 T402E or PAK2 D212N/T402E. Each PAK2 variant was first allowed to autoactivate with [γ-^{32}P] ATP for ten minutes at 30°C. Concentrations of substrate (PAK2 variants) to caspase were varied from a 1:1 to 1:100 ratio. PAK2 cleavage into two fragments (p34 and p27) by casp-7 was assessed after 1 hour by autoradiography. The casp-7 lane is a positive control of casp-7 CTC wild-type with PAK2 T402E in a 1:1 ratio.

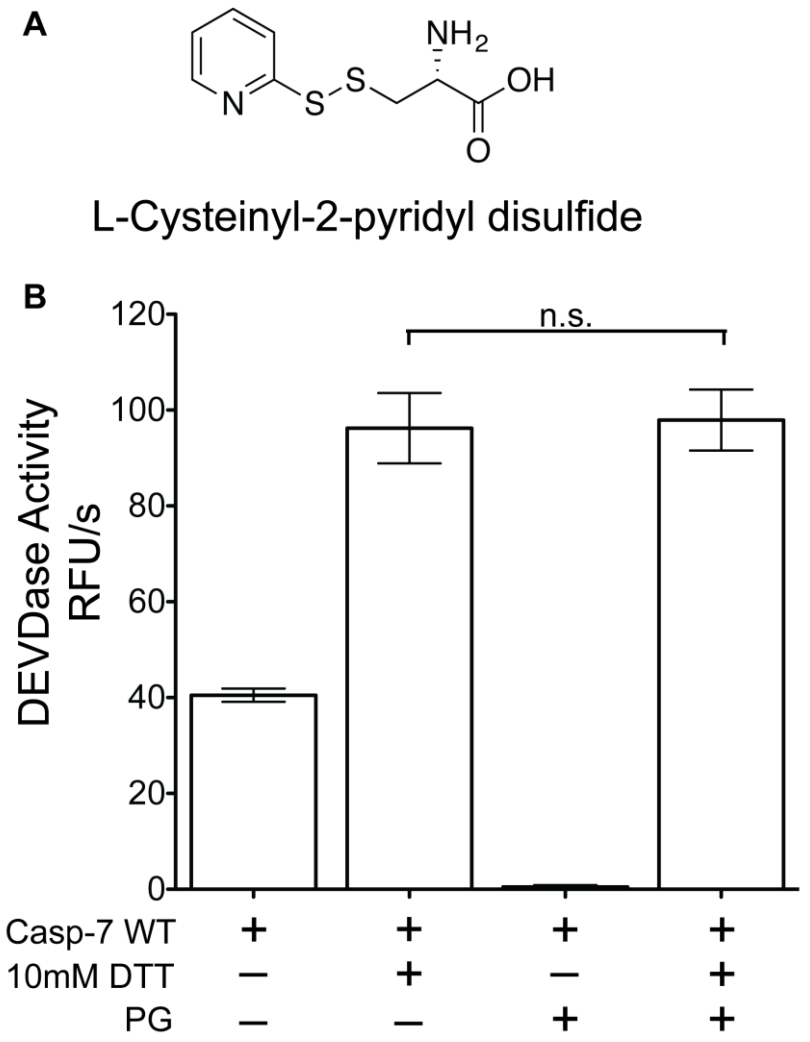

Figure S2. Casp-7 WT can recover full activity after silencing with PG (Related to Figure 2)
(A) Structure of the L-cysteinyl-2-pyridyl disulfide protecting group (PG).
(B) Incubating wild-type casp-7 with 50-fold excess of PG results in a complete loss of activity. This inhibition is fully reversible upon addition of a reducing agent (10mM DTT used here). Unliganded casp-7 (no PG) or liganded casp-7 (plus PG) were treated with 10mM DTT. Casp-7 activity was assessed by monitoring cleavage of the fluorogenic substrate DEVD-AMC. Liganded casp-7 was able to regain full activity with activity (RFU/s) statistically indistinguishable (Student's t test resulted in a P value of >0.05) from untreated casp-7 under the same reducing conditions. Data is represented as mean ± S.D.

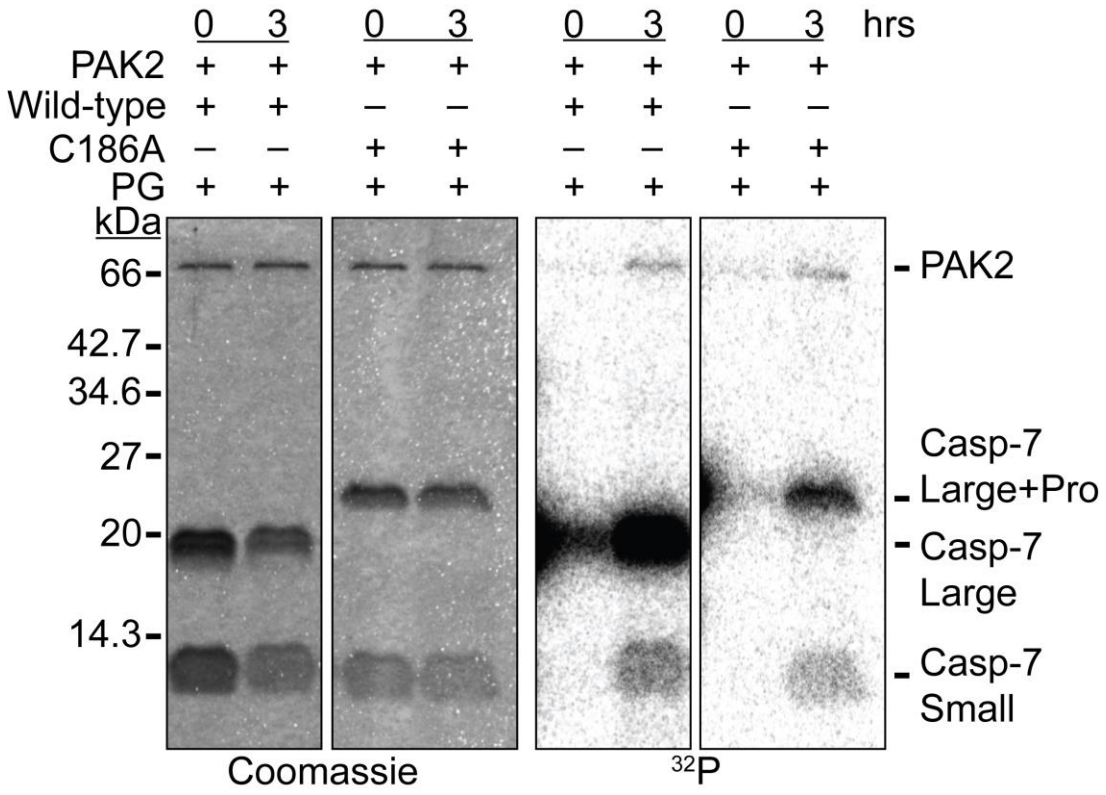

Figure S3. Casp-7 wild-type and C186A are both phosphorylated on the small subunit in the presence of protecting group. (Related to Figure 2)

Both casp-7 wild-type and catalytic knockout (C186A) were reacted with PG and then phosphorylated with preactivated PAK2. Phosphorylation was monitored by autoradiography. The small subunit is phosphorylated in a similar fashion indicating PG binding at C186 is not responsible for PAK2 phosphorylation at S239.

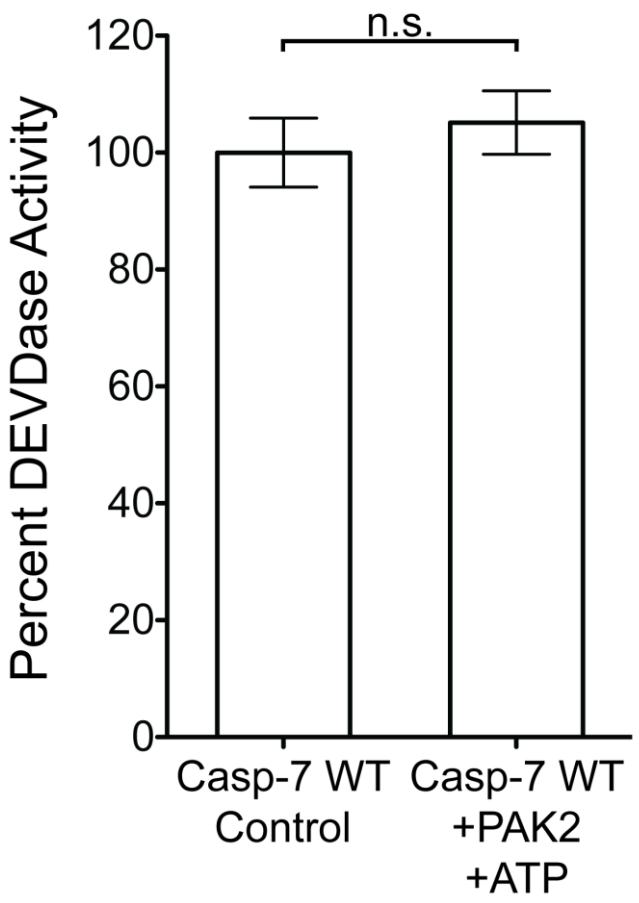

Figure S4. Casp-7 wild-type activity is not affected by PAK2 phosphorylation. (Related to Figure 4)
Casp-7 wild-type CTC was allowed to incubate in PAK2 activity buffer (50mM Tris pH 7.5, 20mM $MgCl_2$, 0.1mM EDTA, 2mM DTT) in the presence and absence of autoactivated PAK2 and 1mM ATP. After a 60 minute incubation at 30°C the activity of the control caspase and the phosphorylated caspase was assessed by monitoring cleavage of the casp-7 fluorogenic peptide substrate DEVD-AMC. Assays were carried out in casp-7 activity assay buffer at 100 nM enzyme concentration. A student's t test resulted in a P value of >0.05 indicating that the control and the phosphorylated casp-7 are statistically identical. Data is represented as mean ± S.D.

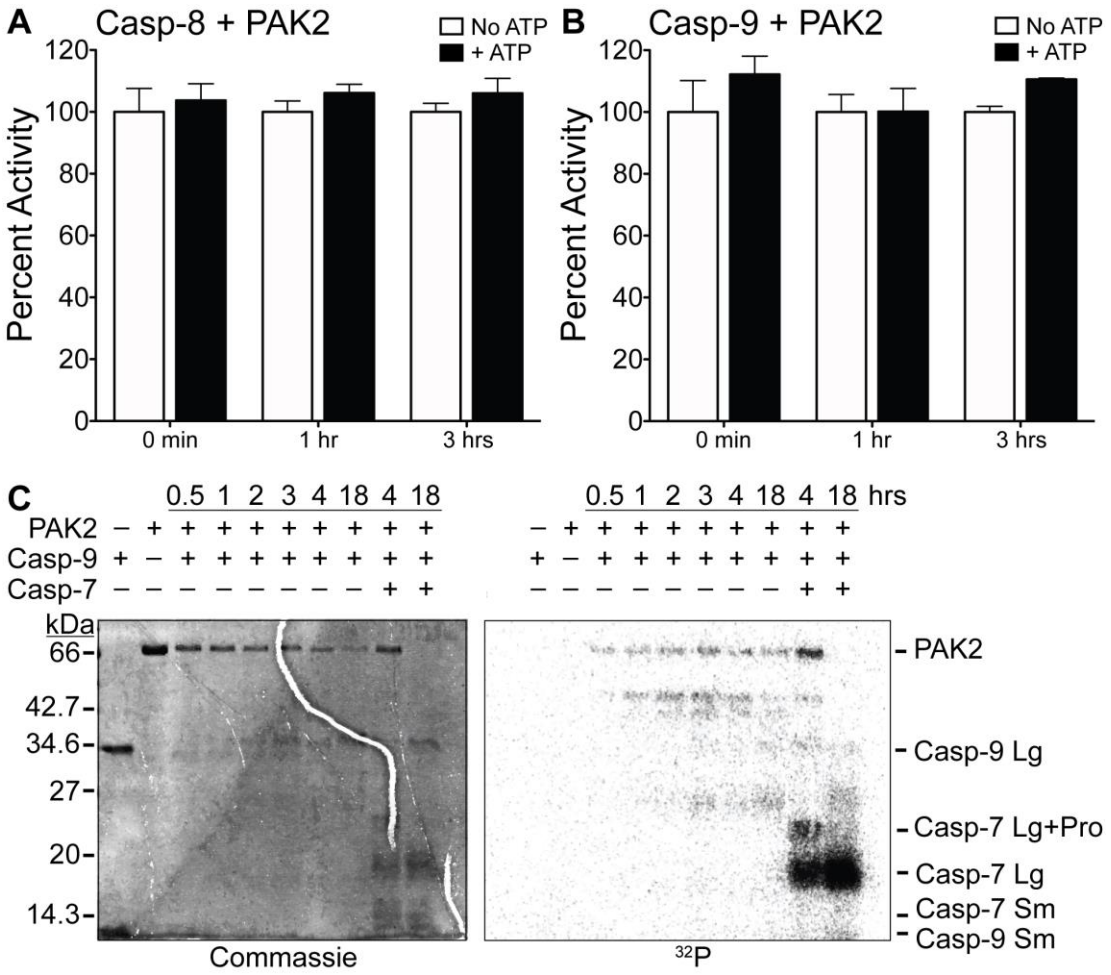

Figure S5: Casp-8 and Casp-9 Activity is Unaffected by PAK2 (Related to Figure 4)
(A) Casp-8 and (B) casp-9 activity was assayed over a ten minute time course monitoring cleavage of the fluorogenic substrate LEHD-AFC. Enzymes were incubated with autoactivated PAK2 T402E (black bars, +ATP) or PAK2 T402E alone (white bars, No ATP) and activity was assessed at three time points. This experiment was performed in identical fashion to the caspase cleavage assays of full-length casp-7 (Figure 4B and 4D). Data is represented as mean ± S.D.
(C) Autoactivated PAK2 was allowed to incubate with casp-9 for up to 18 hours with [γ-^{32}P] ATP. No bands for casp-9 appeared via autoradiography, suggesting PAK2 is unable to phosphorylate casp-9 under these assay conditions. In addition, full length casp-7 was incubated with casp-9 and autoactivated PAK2 for 18 hours as a positive control to demonstrate (i) PAK2 is active because it phosphorylates the large subunit of casp-7 and (ii) that casp-9 is active because it is able to cleave full length casp-7.

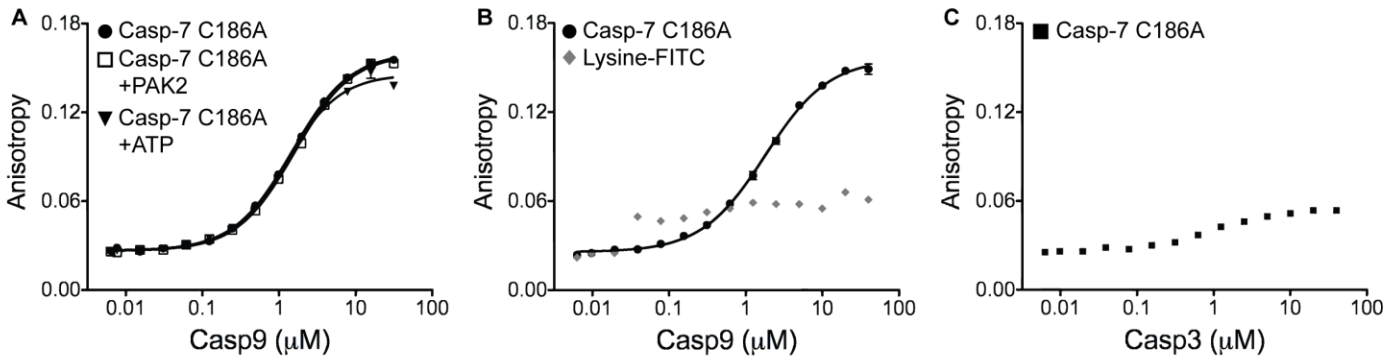

Figure S6: Fluorescence Polarization Controls (Related to Figure 5)

(A) Casp-7 C186A was fluorescently labeled with FITC and fluorescence anisotropy was measured over a casp-9 titration. Casp-7 C186A alone (filled circles), casp-7 C186A incubated in the presence of PAK2 and the absence of ATP (empty squares), and casp-7 C186A with ATP (triangles) all showed overlapping curves indicating addition of these molecules has no effect on casp-7 interacting with casp-9.

(B) Free lysine labeled with FITC was incubated with casp-9 at various concentrations and the fluorescence anisotropy was measured. A constant tumbling was observed even at high casp-9 concentrations, suggesting FITC itself does not interact with casp-9.

(C) Casp-7 C186A was labeled with FITC as before and fluorescence anisotropy was measured over a casp-3 titration. Only a small change in anisotropy was observed, demonstrating that fluorescently labeled casp-7 C186A does not behave in a similar manner with every caspase and has a unique curve with casp-9.

Table S1: Crystallographic data collection and refinement statistics for unliganded casp-7 S239E. (Related to Figure 3)

(D) PDB ID	5K20
Data Collection	
Beamline	NSLS X6A
Resolution Range (Å)	76.98-2.20 (2.24-2.20)
Unique Reflections	43,569
Redundancy	10.9
Completeness (%)	99.53
I/σ (I)	37.4 (1.8)
R_{sym}	0.076
Space Group	$P3_221$
a = b (Å)	88.76
c (Å)	185.14
α = β (°)	90
γ (°)	120
Refinement	
R_{work}/R_{free} (%)	19.1/22.8
Average B Factor (Å^2)	66.3
Residue Range Built	58-198, 211-303
RMSD	
Bond Lengths (Å)	0.017
Bond Angles (°)	1.7659
Ramachandran Plot (%)	
Preferred	95.4
Allowed	4.6
Outliers	0.0

Values in parentheses are for the highest resolution bin.
RMSD, root-mean-square deviation

Supplemental Experimental Procedures

DNA expression constructs and Antibodies

Human caspase-7 (*CASP7*) in pET23b (Zhou et al., 1997) was a gift from Guy Salvesen. Human caspase-9 (*CASP9*) in pET23b (Stennicke et al., 1999) was obtained from Addgene. Human caspase-8 (*CASP8*) in pET15b (Zhou et al., 1997) was a gift from JB Denault. Human p21 activated kinase 2 (*PAK2*) in pET28b was a gift from John Kuriyan. The protecting group (PG, cysteinyl-2-pyridyl disulfide) was synthesized as previously described (Ventura et al., 2015). Dulbecco's modified Eagle's medium (DMEM) and all other cell culture supplements were purchased from Gibco (Life Technologies). The pLX304 vector containing the caspase-7 (*CASP7*) for transient transfections was obtained from Harvard Plasmid. The caspase-7 antibody for detecting the large subunit and the HDAC-1 antibody were purchased from Cell Signaling Technologies.

Caspase-7 Expression and Purification

Plasmids encoding human caspase-7 (*CASP7*) and all variants were transformed into BL21(DE3) *E. coli* cells. Cultures were grown in 2xYT media with ampicillin (100 μg/mL, ThermoFisher) at 37°C until they reached an OD_{600} of 0.6. The temperature was reduced to 18°C and cells were induced with 1 mM Isopropyl β-D-1-thiogalactopyranoside (IPTG) for 18 hours. Cell pellets were stored at -80°C, freeze-thawed and lysed in a microfluidizer (Microfluidics, Inc.) in a buffer containing 50 mM sodium phosphate pH 8.0, 300 mM NaCl, and 2 mM imidazole. Lysed cells were centrifuged at 27,000 rcf to remove cellular debris. The supernatant was loaded onto a 5 mL HiTrap Ni-affinity column (GE Healthcare). The column was washed with a buffer of 50 mM sodium phosphate pH 8.0, 300 mM NaCl, and 50 mM imidazole. Caspase-7 was eluted with a step gradient to 300 mM imidazole. The eluted fraction was diluted 6-fold into a buffer containing 20 mM Tris pH 8.5 and 2 mM DTT to reduce the salt concentration. This protein was loaded onto a 5 mL HiTrap Q column (GE Healthcare). The column was developed with a linear NaCl gradient. Protein eluted in 120 mM NaCl and was assessed for purity by SDS-PAGE and stored at -80°C in elution buffer.

For several sets of experiments it was imperative that the caspase-7 retained its full-length uncleaved zymogen form, however, during expression in *E. coli* the prodomain is cleaved off over time. Therefore, full-length caspase-7 was induced for only 10 min at 37°C before harvesting the cells.

Caspase-8 Expression and Purification

The expression construct encoding human caspase-8 (*CASP8*) was transformed into BL21(DE3) *E. coli* cells. Cultures were grown in 2xYT media with ampicillin (100 μg/mL, ThermoFisher) at 37°C until they reached an OD_{600} of 0.6. The temperature was reduced to 25°C and cells were induced with 1 mM Isopropyl β-D-1-thiogalactopyranoside (IPTG) for 3 hours. Cell pellets were stored at -80°C, freeze-thawed and lysed in a microfluidizer (Microfluidics, Inc.) in a buffer containing 50 mM sodium phosphate pH 8.0, 500 mM NaCl, and 2 mM imidazole. Lysed cells were centrifuged at 27,000 rcf to remove cellular debris. The supernatant was loaded onto a 5 mL HiTrap Ni-affinity column (GE Healthcare). The column was washed with a buffer of 50 mM sodium phosphate pH 8.0, 500 mM NaCl, and 8 mM imidazole. Caspase-8 was eluted with a step gradient to 300 mM imidazole. The eluted fraction was diluted 6-fold into a buffer containing 20 mM Tris pH 8.5 and 2 mM DTT to reduce the salt concentration. This sample was loaded onto a 5 mL HiTrap Q column (GE Healthcare). The column was developed with a linear NaCl gradient. Caspase-8 eluted in 120 mM NaCl and was assessed for purity by SDS-PAGE and stored at -80°C in elution buffer.

Caspase-9 Expression and Purification

An expression construct for full-length human caspase-9 (*CASP9*) was transformed into BL21 (DE3) *E. coli* cells. The cultures were grown in 2xYT media with ampicillin (100 μg/mL, ThermoFisher) at 37°C until they reached an OD_{600} of 0.9. The temperature was reduced to 15°C and cells were induced with 1 mM IPTG to express soluble His-tagged caspase-9. Cells were harvested after 3 hrs to obtain single site processing at D315 (Huber and Hardy, 2012). Cell pellets stored at -80°C were freeze-thawed and lysed in a microfluidizer (Microfluidics, Inc.) in 50 mM sodium phosphate pH 8.0, 300 mM NaCl, 2 mM imidazole. Lysed cells were centrifuged at 27,000 rcf to remove cellular debris. The filtered supernatant was loaded onto a 5 mL HiTrap Ni-affinity column (GE Healthcare). The column was washed with 50 mM sodium phosphate pH 8.0, 300 mM NaCl, 2 mM imidazole until the absorbance returned to baseline. The protein was eluted using a 2-100 mM imidazole gradient over the course of 270 mL. The eluted fractions containing protein of the expected molecular weight and composition were diluted 10-fold into a buffer containing 20 mM Tris pH 8.5 and 5 mM DTT to reduce the salt concentration. This caspase-9 sample was loaded onto a 5 mL HiTrap Q column (GE Healthcare). The column was developed with a linear NaCl gradient and

eluted in a buffer containing 20 mM Tris pH 8.5, 180 mM NaCl, and 5 mM DTT. The eluted protein was stored at -80°C in the elution buffer and was analyzed by SDS-PAGE for purity.

PAK2 T402E Expression and Purification

An expression construct for human p21 activated kinase 2 (*PAK2*) T402E was transformed into BL21(DE3) *E. coli* cells. Cultures were grown in 2xYT media with kanamycin (40 μg/mL, ThermoFisher) at 37°C until they reached an OD_{600} of 0.6. The temperature was reduced to 25°C and cells were induced with 1 mM Isopropyl β-D-1-thiogalactopyranoside (IPTG) for 3 hours. Cell pellets were stored at -80°C, freeze-thawed and lysed in a microfluidizer (Microfluidics, Inc.) in a buffer containing 50 mM sodium phosphate pH 8.0, 300 mM NaCl, 0.05% Tween-20, and 2 mM imidazole. Lysed cells were centrifuged at 27,000 rcf to remove cellular debris. The supernatant was loaded onto a 5 mL HiTrap Ni-affinity column (GE Healthcare). The column was washed with a buffer of 50 mM sodium phosphate pH 8.0, 300 mM NaCl, 0.05% Tween-20, and 10 mM imidazole. PAK2 was eluted with a step gradient to 300 mM imidazole. The eluted fraction was diluted 6-fold into a buffer containing 20 mM Tris pH 8.5 and 2 mM DTT, to reduce the salt concentration. This protein sample was then loaded onto a 5 mL HiTrap Q column (GE Healthcare). The column was developed with a linear NaCl gradient. Protein eluted in 120 mM NaCl and was assessed for purity by SDS-PAGE and stored at -80°C in elution buffer.

Generation of Caspase-7 Variants

All wild-type and mutant versions of caspase-7 were expressed from a pET23b vector with a carboxy-terminal His_6-tag. The full-length caspase-7 construct encodes residues 1-303, while a constitutively-two-chain corrected (CTC) construct was designed to produce the large (1-198) and small (199-303) subunits of caspase-7 as two independent polypeptides. All variants that were generated in either construct were created using QuikChange (Stratagene) site-directed mutagenesis. All DNA sequences were verified by DNA sequencing (Genewiz).

Caspase-7 S239E Crystallization and Data Collection

Purified caspase-7 S239E (CTC construct) in a buffer containing 120 mM NaCl and 20 mM Tris buffer, pH 8.0, was concentrated using Millipore Ultrafree 3K NMWL membrane concentrators (Millipore) to 18 mg/mL as assessed by absorbance at 280 nm. Crystal trays were setup at room temperature and grown in 3 μL hanging drop trays with mother liquor consisting of 2.1 M sodium formate and 300 mM sodium citrate, pH 5.5, in a 2:1 ratio of protein to mother liquor. Crystals grew to a maximum of 240 μm × 340 μm in 3 days at 20°C. Crystals were cryoprotected in 20% ethylene glycol in mother liquor with a 60 second incubation, and then frozen by rapid immersion in liquid N_2. Diffraction data was collected at Brookhaven National Laboratories National Synchrotron X6A beamline (Upton, NY).

Structure Determination

X-ray data was indexed, integrated, and scaled using HKL2000 software (Otwinowski and Minor, 1997) and well defined diffraction spots were observed to 2.2 Å. Crystallographic phases were generated by molecular replacement using 3IBF as a search model for PhaserMR (McCoy et al., 2007), part of the CCP4 software suite (Winn et al., 2011). To avoid bias, substrate binding loops were omitted from the search model and rebuilt into unambiguous electron density. Structures were refined using iterative rounds of rebuilding in Coot (Emsley et al., 2010) and refinement in Refmac5 (Murshudov et al., 1997) using individual B-factors. Water and formate molecules were modeled into the structures, verified with refinement, and checked by stereo-chemical viability. A final round of refinement with NCS restraints imposed was performed in Phenix (Adams et al., 2010).

Activity Assays

For kinetic measurements of caspase activity, 100 nM freshly purified protein was assayed over the course of 7 minutes in a caspase-7 activity-assay buffer containing 100 mM HEPES pH 7.5, 5 mM $CaCl_2$, 10% PEG 400, 0.1% CHAPS, and 5 mM DTT. For substrate titrations, a range of 0-200 μM of the fluorogenic substrate DEVD-AMC, (N-acetyl-Asp-Glu-Val-Asp-AMC (7-amino-4-methylcoumarin), Enzo Lifesciences; Ex. 365 nm / Em. 495 nm), was added to initiate the reaction. Assays were performed in triplicate at 37°C in 100 μL volumes in 96-well microplate format using a Molecular Devices Spectramax spectrophotometer. Initial velocities versus substrate concentration were fit to a rectangular hyperbola using GraphPad Prism (Graphpad Software) to determine the kinetic parameters K_M and k_{cat}. Enzyme concentrations were determined by active-site titrations with the quantitative inhibitor DEVD-CHO (N-Acetyl-Asp-Glu-Val-Asp-Aldehyde; Enzo Lifesciences) or z-VAD-FMK (Z-Val-Ala-Asp-fluoromethylketone; Enzo Lifesciences). Active-site titrations were incubated over a period of 2 hours in activity assay buffer. Optimal labeling was observed when protein was added to DEVD-CHO or z-VAD-FMK

solvated in DMSO in 96-well V-bottom plates, sealed with tape, and incubated at room temperature in a final volume of 200 μL. 90 μL aliquots were transferred to black-well plates in duplicate and assayed with 50-fold molar excess of substrate. The protein concentration was determined to be the lowest concentration of DEVD-CHO or z-VAD-FMK inhibitor at which full inhibition was observed.
Caspase-8 and caspase-9 kinetics were assessed as described above, using the peptide substrate LEHD-AFC (N-acetyl-Leu-Glu-His-Asp-AFC (7-amino-4-trifluoromethylcoumarin), Enzo Life Sciences; Ex. 380 nm/ Em. 505 nm). In addition each assay was performed in the enzyme's preferred activity assay buffer (see Materials and Methods).

Cell Culture and Transfection
MCF7 breast cancer cells were cultured in Dulbecco's modified Eagle medium (DMEM) supplemented with 10% fetal bovine serum, 4.5 g/L D-glucose, 1 mM sodium pyruvate, 100 mg/mL streptomycin, 100 units/mL penicillin, and 1% Glutamax. Cells were incubated at 37°C in a humidified atmosphere maintained at 5% CO_2. Cells were transiently transfected using Lipofectamine 3000 (Invitrogen) according to the manufacturer instructions. Transfection was assessed by comparative immunoblotting of transfected and non-transfected cells.

Immunoblotting
Cellular proteins from transfected MCF lysates were first separated by SDS-PAGE. Each well of a 12% acrylamide gel was loaded with 20 μg of total protein from lysates. Proteins were then electrotransferred onto a polyvinylidene difluoride (PVDF) membrane. The membranes were washed overnight in a 3% BSA blocking solution containing Tris-buffered saline with 0.1% Tween-20. The following day the membrane was probed with primary antibodies. Both the caspase-7 antibody (recognizing the large subunit) and the HDAC-1 antibody (loading control) were obtained from Cell Signaling Technologies. Antibody-antigen complexes were then washed and blotted with goat anti-rabbit IgG-peroxidase conjugates (Jackson ImmunoResearch Labs). After a final washing in TBST, the membrane was introduced to the enhanced chemiluminescent substrate for horseradish peroxidase (HRP) and detected according to the manufacturer's instructions (ThermoFisher Kit) using a ChemiDocMP (Biorad Laboratories Inc.).

Supplemental References

Adams, P.D., Afonine, P. V., Bunkóczi, G., Chen, V.B., Davis, I.W., Echols, N., Headd, J.J., Hung, L.W., Kapral, G.J., Grosse-Kunstleve, R.W., et al. (2010). PHENIX: A comprehensive Python-based system for macromolecular structure solution. Acta Crystallogr. Sect. D Biol. Crystallogr. *66*, 213–221.

Emsley, P., Lohkamp, B., Scott, W.G., and Cowtan, K. (2010). Features and development of Coot. Acta Crystallogr. Sect. D Biol. Crystallogr. *66*, 486–501.

Huber, K.L., and Hardy, J.A. (2012). Mechanism of zinc-mediated inhibition of caspase-9. Protein Sci. *21*, 1056–1065.

McCoy, A.J., Grosse-Kunstleve, R.W., Adams, P.D., Winn, M.D., Storoni, L.C., and Read, R.J. (2007). Phaser crystallographic software. J. Appl. Crystallogr. *40*, 658–674.

Murshudov, G.N., Vagin, A.A., and Dodson, E.J. (1997). Refinement of macromolecular structures by the maximum-likelihood method. Acta Crystallogr. Sect. D Biol. Crystallogr. *53*, 240–255.

Otwinowski, Z., and Minor, W. (1997). Processing of X-ray diffraction data collected in oscillation mode. Methods Enzymol. *276*, 307–326.

Stennicke, H.R., Deveraux, Q.L., Humke, E.W., Reed, J.C., Dixit, V.M., and Salvesen, G.S. (1999). Caspase-9 can be activated without proteolytic processing. J. Biol. Chem. *274*, 8359–8362.

Ventura, J., Eron, S.J., González-Toro, D.C., Raghupathi, K., Wang, F., Hardy, J.A., and Thayumanavan, S. (2015). Reactive Self-Assembly of Polymers and Proteins to Reversibly Silence a Killer Protein. Biomacromolecules *16*, 3161–3171.

Winn, M.D., Ballard, C.C., Cowtan, K.D., Dodson, E.J., Emsley, P., Evans, P.R., Keegan, R.M., Krissinel, E.B., Leslie, A.G.W., McCoy, A., et al. (2011). Overview of the CCP4 suite and current developments. Acta Crystallogr. Sect. D Biol. Crystallogr. *67*, 235–242.

Zhou, Q., Snipas, S., Orth, K., Muzio, M., Dixit, V.M., and Salvesen, G.S. (1997). Target Protease Specificity of the Viral Serpin CrmA: Analysis of the five Caspases. J. Biol. Chem. *272*, 7797–7800.